



**The Abdus Salam
International Centre for Theoretical Physics**



2155-33

International Workshop on Cutting-Edge Plasma Physics

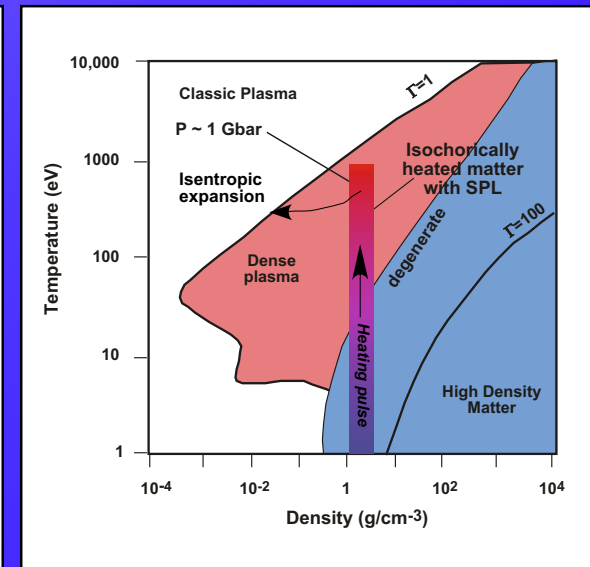
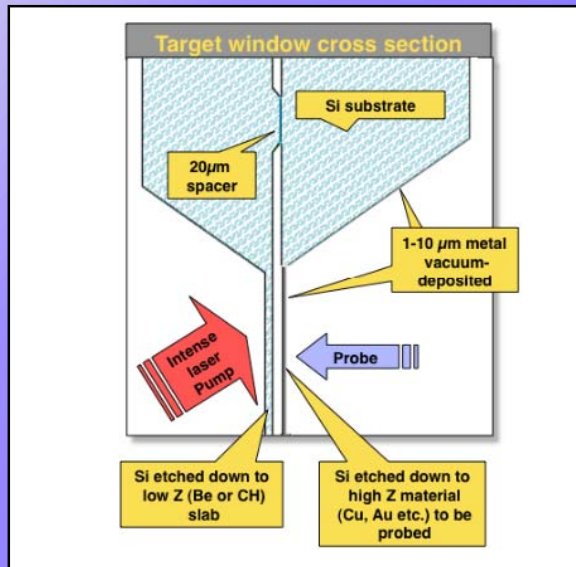
5 - 16 July 2010

High Energy Density Science

Todd Ditmire

*Texas Center for High Intensity Laser Science
Department of Physics
University of Texas at Austin
USA*

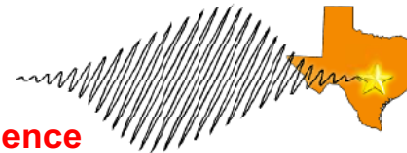
High Energy Density Science



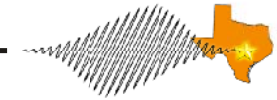
Presented by:

Todd Ditmire

**Texas Center for High Intensity Laser Science
Department of Physics
University of Texas at Austin**

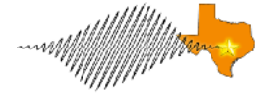


“High Energy Density Physics” can be roughly defined as study of matter at energy density 10^{11} J/m^3

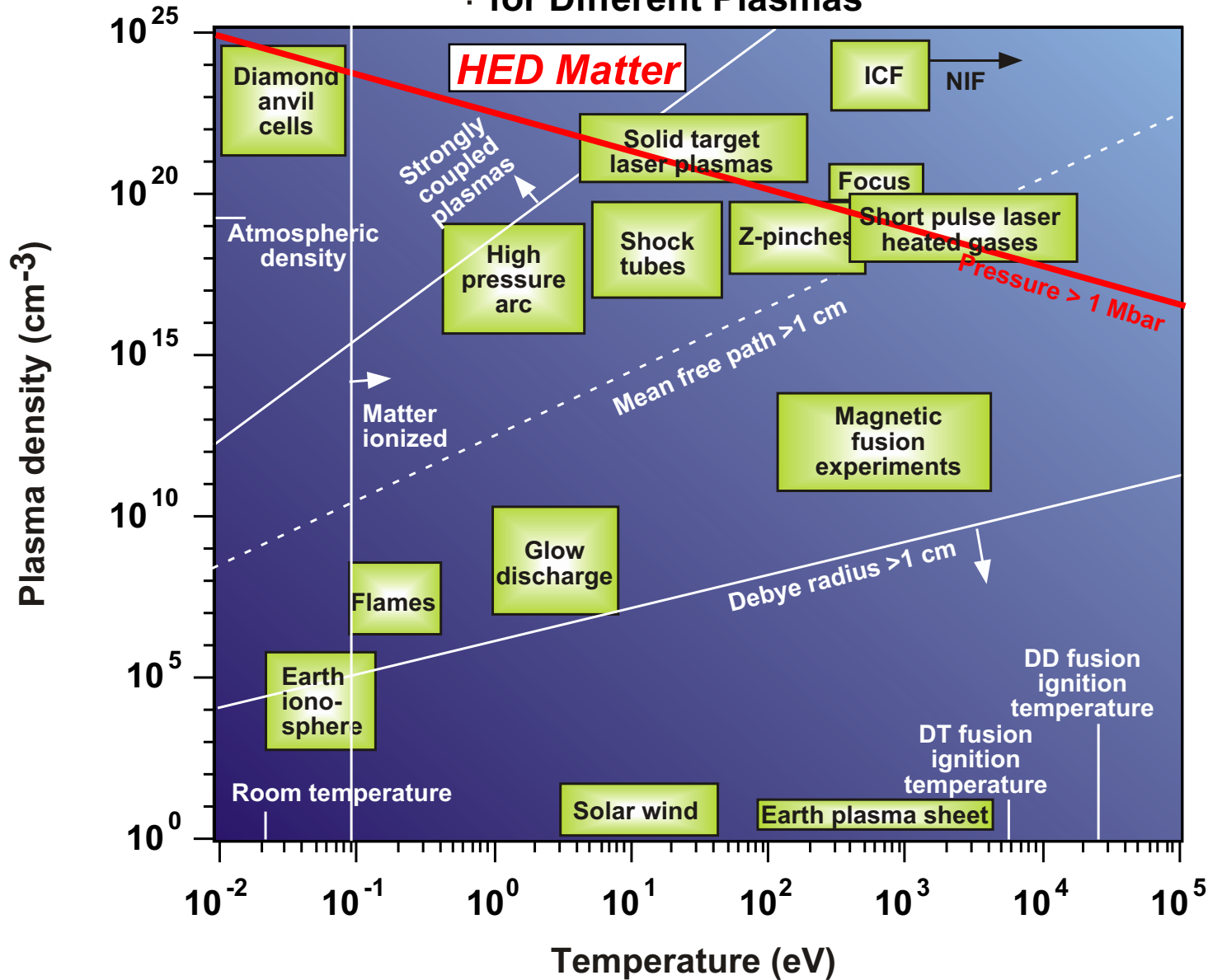


High Energy Density Parameter	Value yielding equivalent to 1 Mbar – Energy density of 10^{11} J/m^3
Plasma density with $T = 1 \text{ keV}$ (10^7 K)	$6 \times 10^{20} \text{ cm}^{-3}$
Plasma temp at solid density ($n \approx 10^{23} \text{ cm}^{-3}$)	6 eV
Electromagnetic wave intensity	$3 \times 10^{15} \text{ W/cm}^2$
Electric field strength	$1.5 \times 10^{11} \text{ V/m}$
Magnetic field strength	500 T
Blackbody radiation temperature	400 eV
Current density for 100 MeV electrons	30 MA/cm^2
Laser intensity to yield 1 Mbar ablation pressure	$4 \times 10^{12} \text{ W/cm}^2$

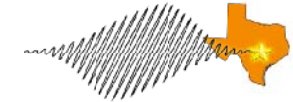
High energy density matter is created by heating dense plasma to very high temperature



Temperature and Density Conditions for Different Plasmas



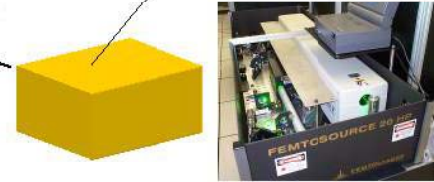
Most modern ultraintense lasers are based on Chirped Pulse Amplification



2) Using gratings, the pulse is stretched by 10,000 x



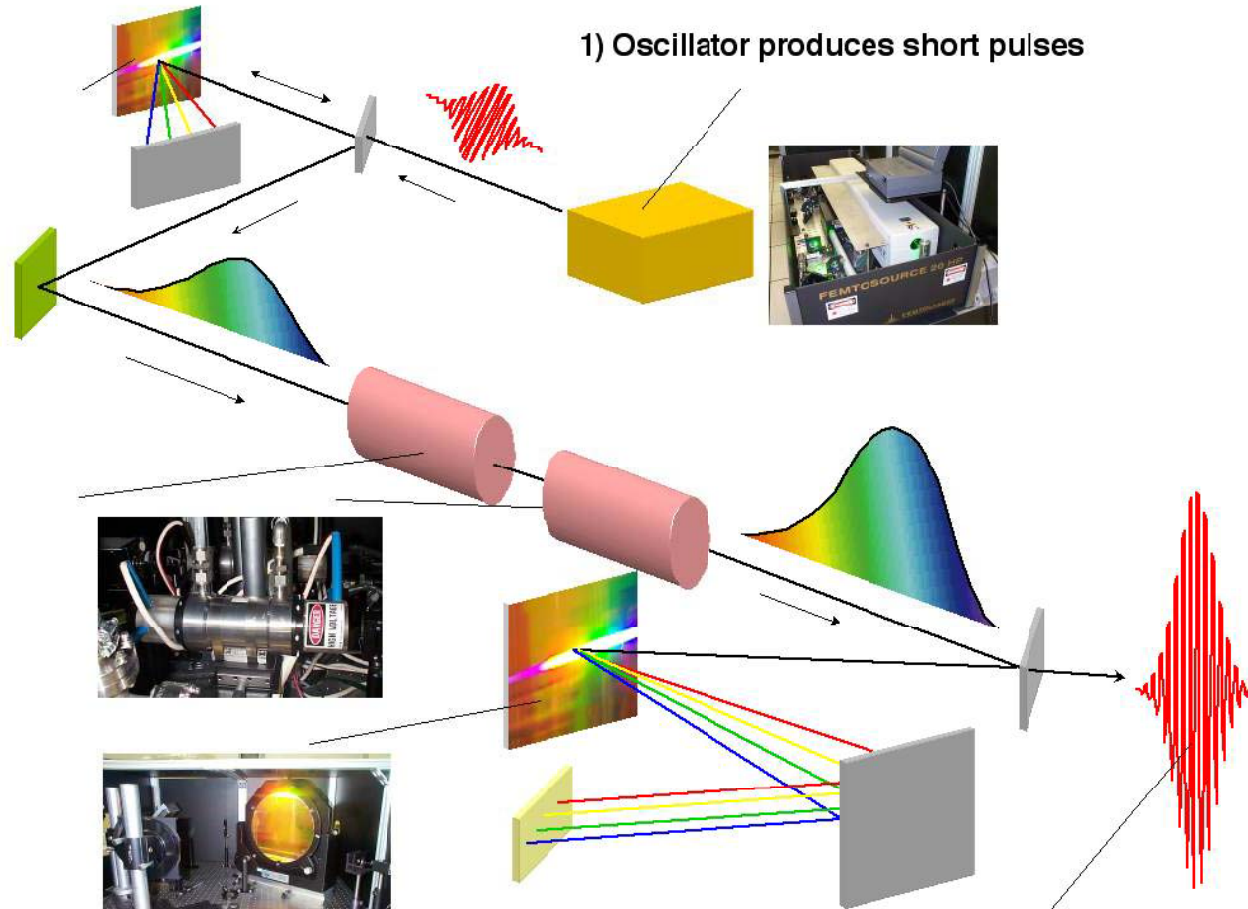
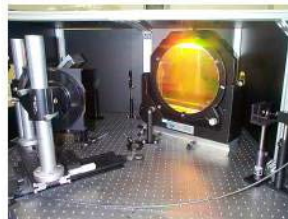
1) Oscillator produces short pulses



3) Long pulses are now safe to amplify in laser amplifiers



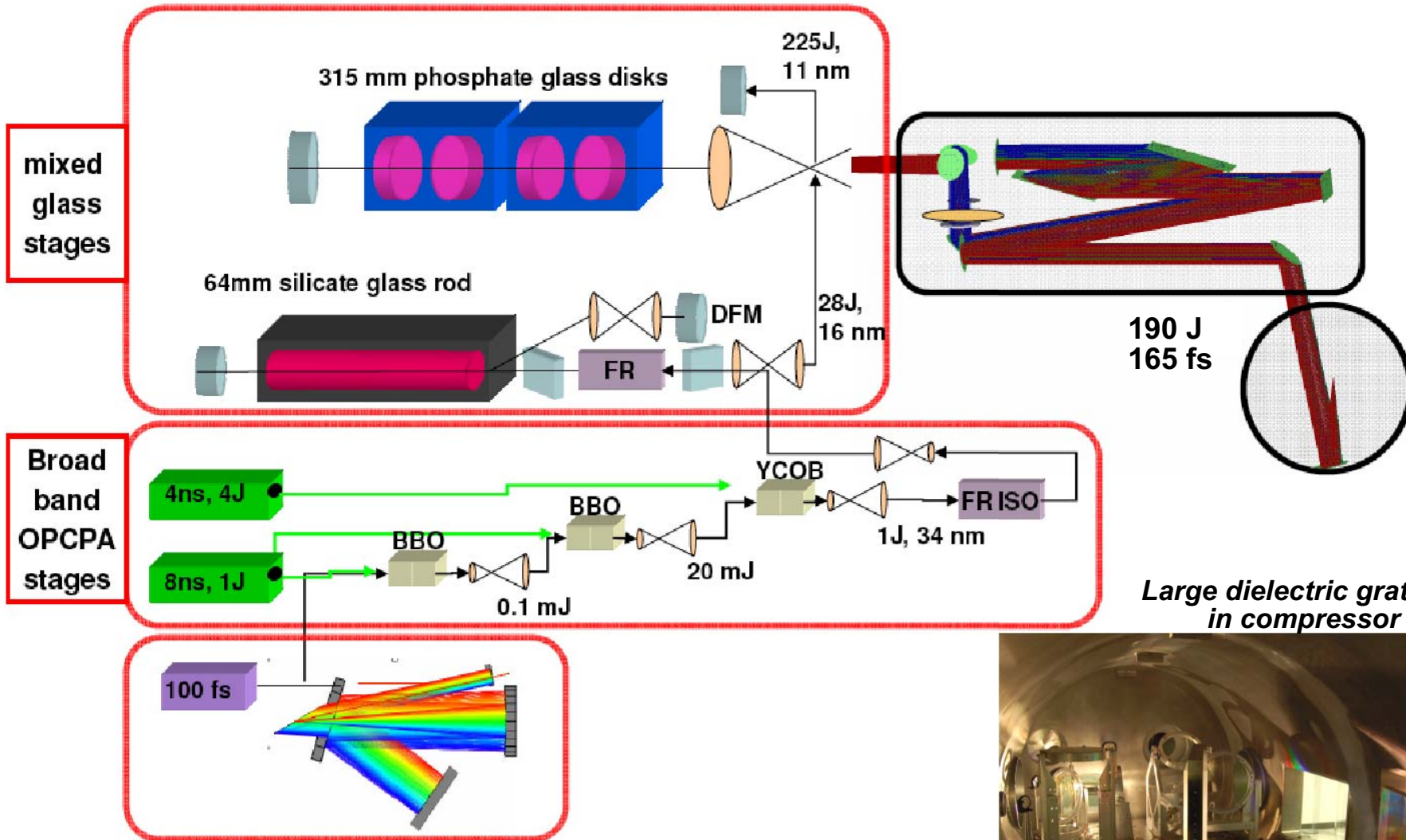
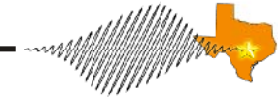
4) After amplification, the pulses are recompressed with gratings



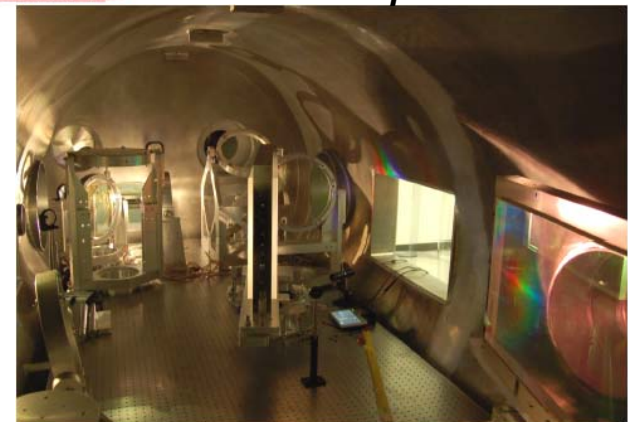
Resulting pulse is short (20-1000 fs) and high energy 1 mJ - 1 kJ

• Strickland and Mourou *Opt. Comm.* 56, 219 (1985)

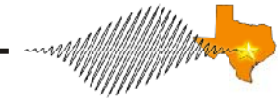
The Texas Petawatt design is based on a 3-stage OPCPA amp and a mixed glass chain



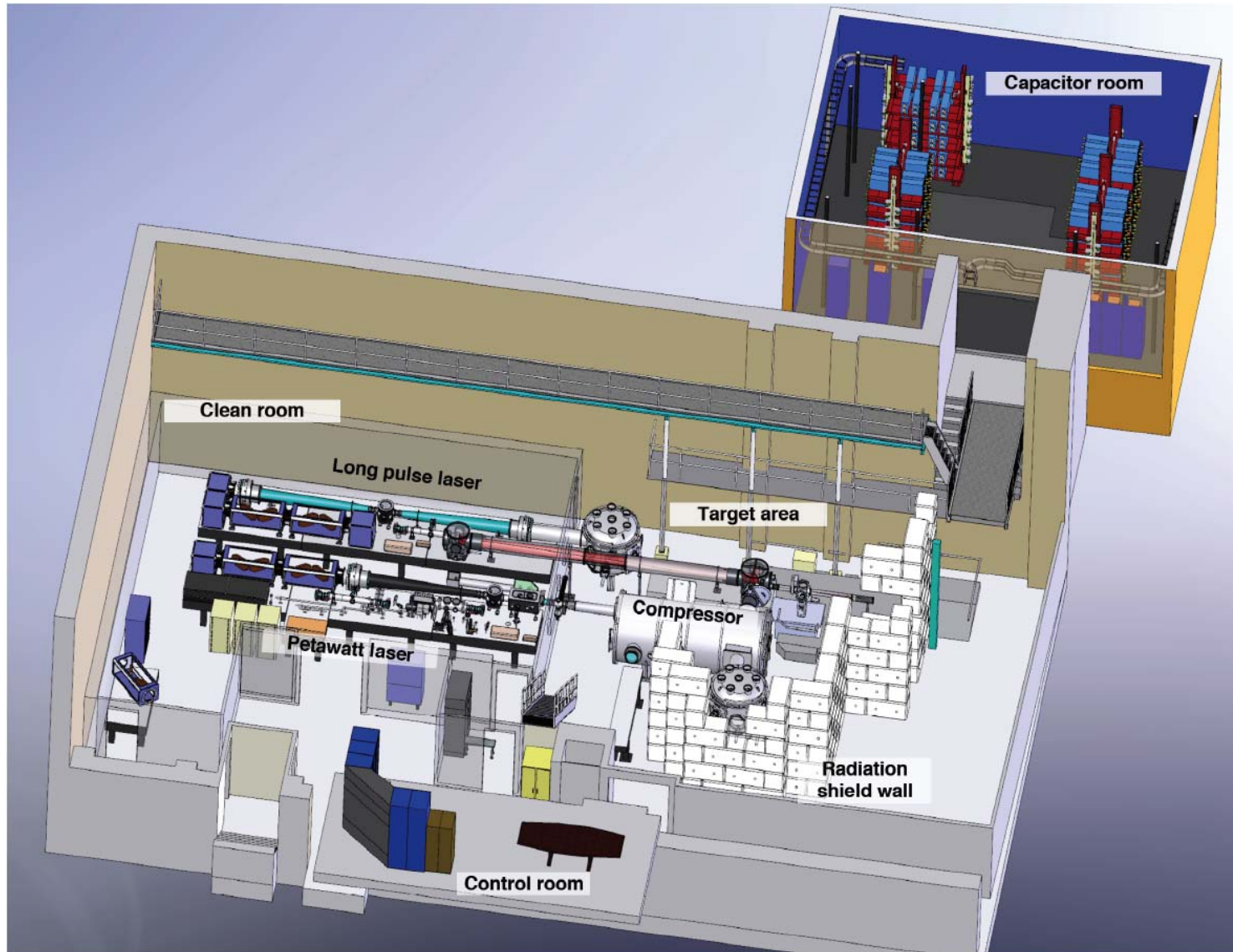
Large dielectric gratings in compressor



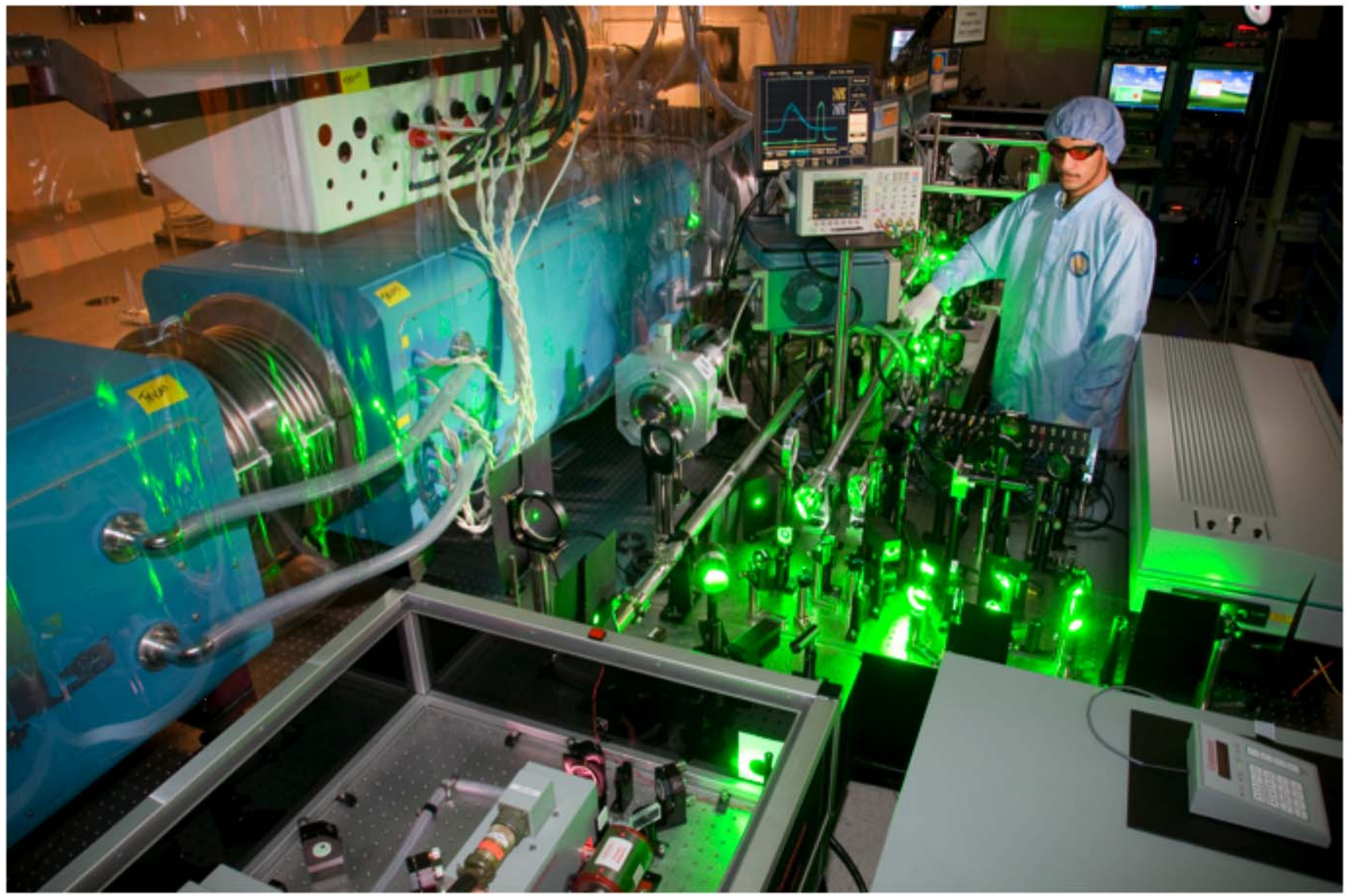
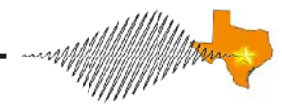
The Texas Petawatt Laser is housed in the RLM High Bay



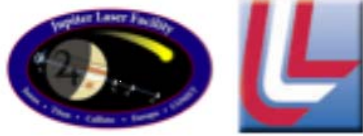
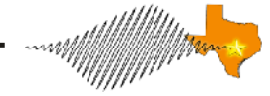
Layout of the Texas Petawatt Facility in the Robert Lee Moore Basement



The Texas PW is a compact CPA laser operating with compressed energy of 190 J



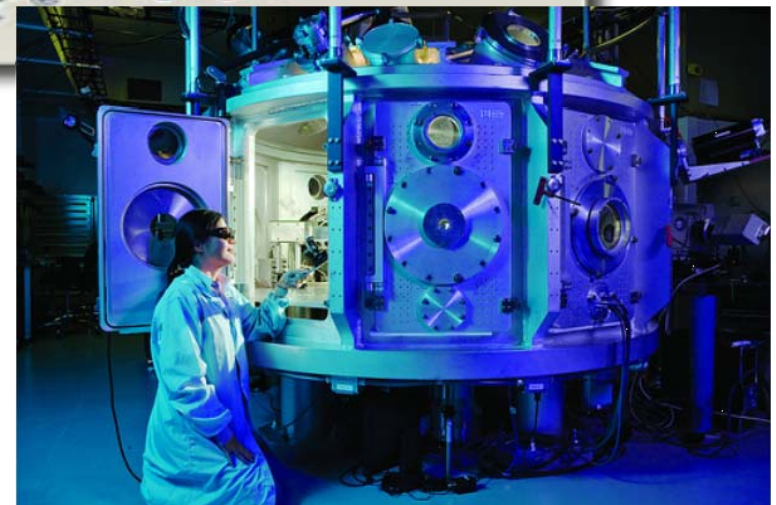
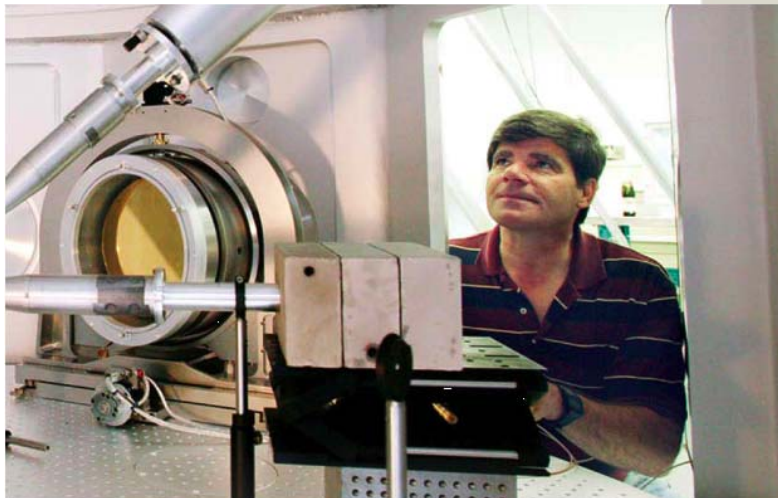
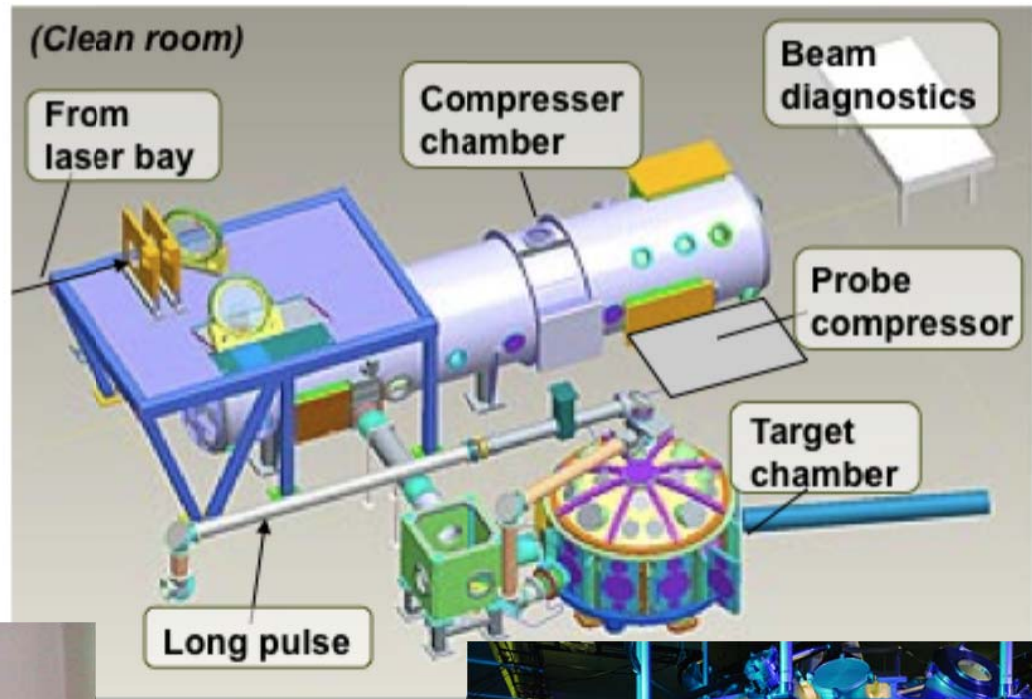
The Titan laser at LLNL is a 250 TW Nd:glass laser devoted to HED research



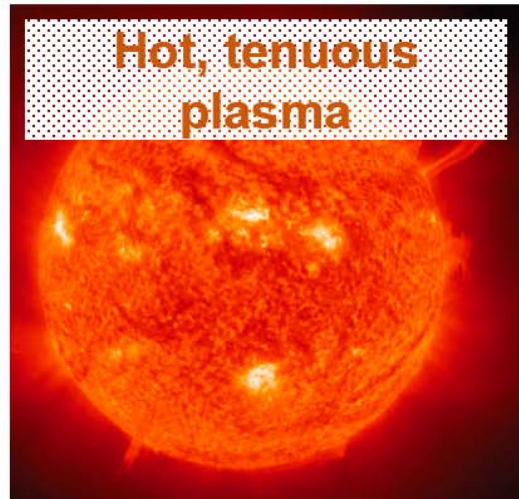
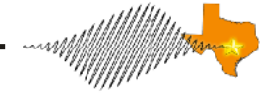
Titan parameters

OPCPA glass 1054 nm

- 150 J (future: 400 J)
- 600 fs (future: 400 fs)
- Up to 5 shots per day (future: 3)
(contingent on rad. safety)
- kJ long pulse beam



A quantitative understanding of these HED plasma physics issues is of considerable practical importance



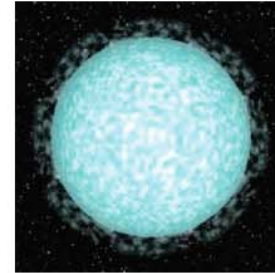
Hot, tenuous plasma



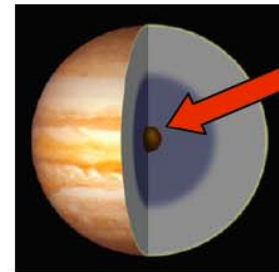
Hot dense matter



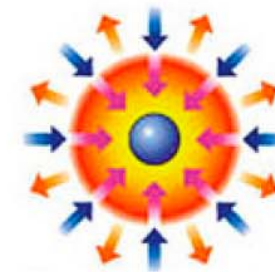
Condensed matter



White dwarfs

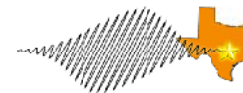


Cores of giant planets and brown dwarfs



Fusion fuel capsule compression

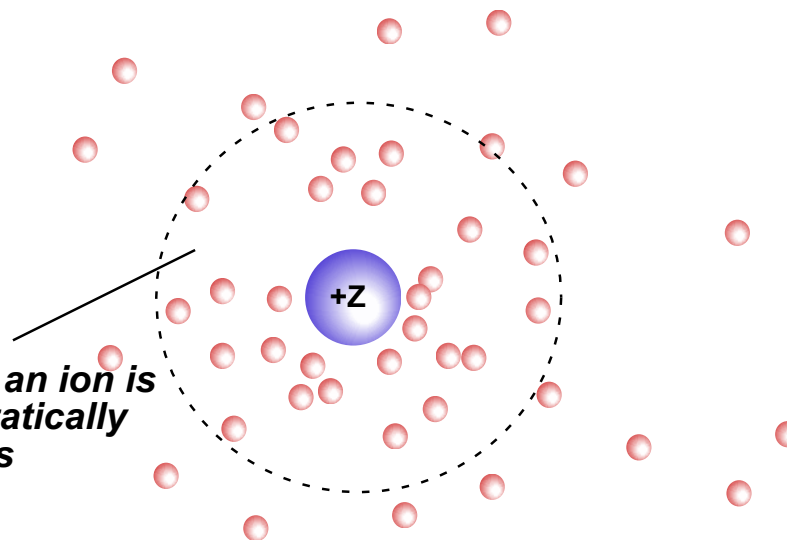
HED plasmas exhibit significant differences to classic, tenuous plasmas



Debye length

$$\lambda_D = \sqrt{\frac{kT_e + kT_i}{4\pi e^2 Z n_o}}$$

Distance over which an ion is a plasma is electrostatically shielded by electrons



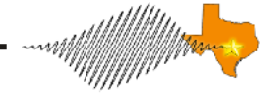
Plasma Parameter

$$\Lambda_p = \frac{1}{\sqrt{Z n_o}} \left(\frac{kT_e}{4\pi e^2} \right)^{3/2}$$

Number of electrons within a sphere with radius of the Debye length - determines if shielding picture is appropriate concept

<u>Tokamak plasma</u>	<u>HED plasma</u>
$kT_e = 10 \text{ keV}$	$kT_e = 100 \text{ eV}$
$n_e = 10^{14} \text{ cm}^{-3}$	$n_e = 10^{22} \text{ cm}^{-3}$
$\Lambda_p = 4 \times 10^7$	$\Lambda_p = 4$

From a "plasma point-of-view", HED matter can not be described by classical, two-body interactions



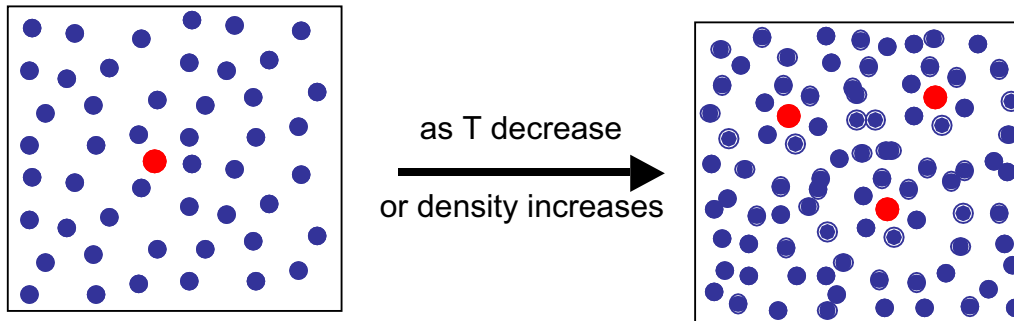
- In "classic" plasmas; $\Gamma < 1$
 - Particles treated as point charges
 - Two body interactions dominate kinetics
- At high density and temperature; $\Gamma > 1$:
 - Particle correlations become important
 - Ionization potentials are depressed
 - Energy levels shift

- Γ is the strong coupling parameter: ratio of the interaction energy between the particles, V_{ii} , to the kinetic energy, T

$$\Gamma = \frac{V_{ii}}{k_B T} = \frac{Z^2 e^2}{r_0 k_B T}$$

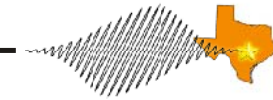
where $r_0 \propto \frac{1}{\rho^{1/3}}$

Classic Cluster expansion (BBGKY hierarchy) leading to usual kinetic equations (Vlasov; Fokker-Planck) is not valid

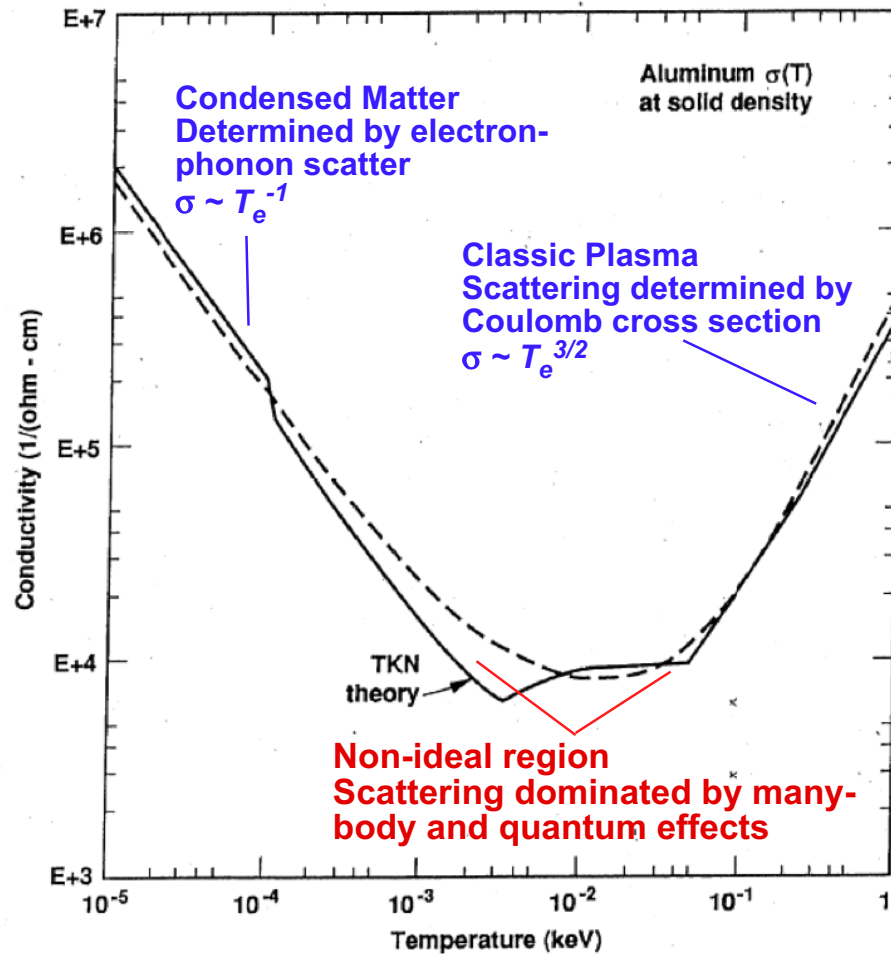


Solid aluminum is strongly coupled to temperature of >500 eV

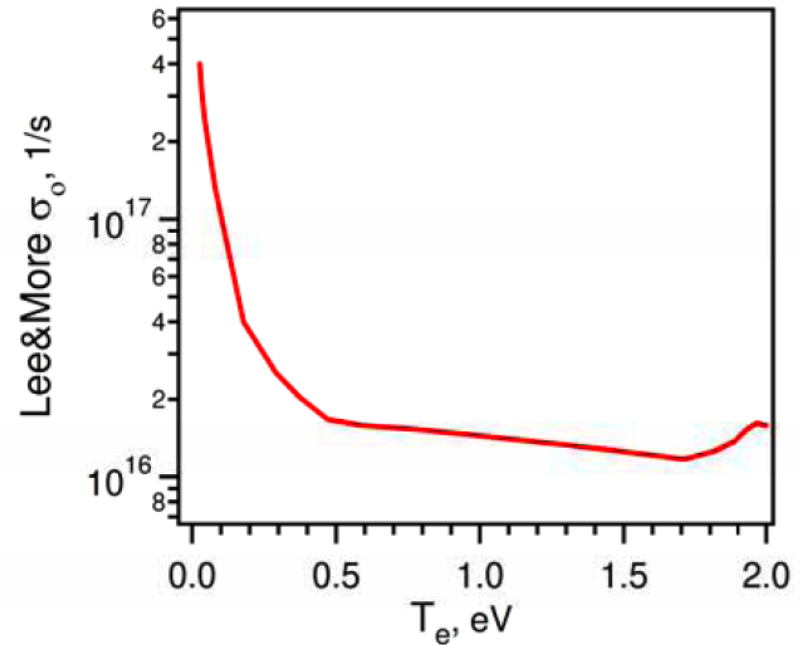
The conductivity of a warm-dense strongly coupled plasma differs significantly from an ideal plasma



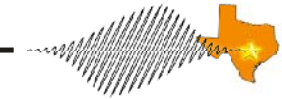
Calculated conductivity of solid Al vs. Temperature



Commonly used model for the conductivity of solid Al



Having a precise equation of state is critical for modeling many phenomena



Pure hydrodynamics can be described accurately by the Euler equations

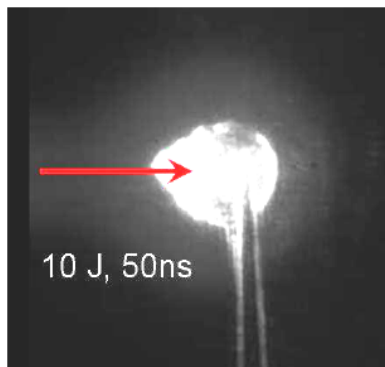
Conservation of mass:
$$\frac{\partial \rho}{\partial t} + \nabla \cdot (\rho \mathbf{v}) = 0$$

Conservation of momentum:
$$\frac{\partial \mathbf{v}}{\partial t} + (\mathbf{v} \cdot \nabla) \mathbf{v} = -\frac{\nabla p}{\rho}$$

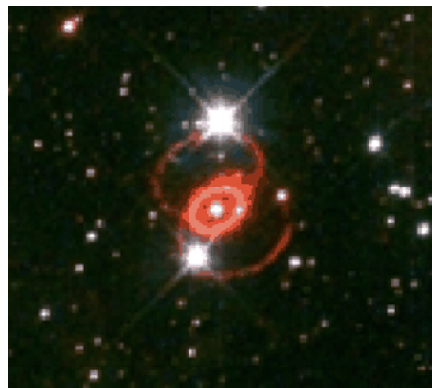
Conservation of entropy:
$$\frac{\partial p}{\partial t} - \gamma \frac{p}{\rho} \frac{\partial \rho}{\partial t} + \mathbf{v} \cdot \nabla p - \gamma \frac{p}{\rho} \mathbf{v} \cdot \nabla \rho = 0$$

EOS

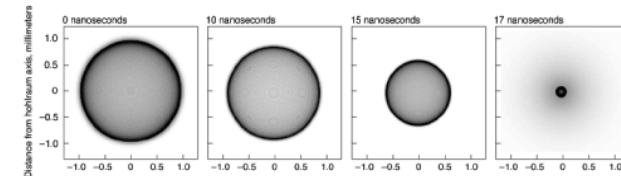
Laser heated plasma expansion



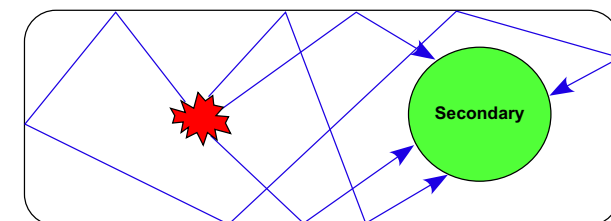
Super novae explosion



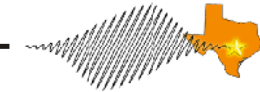
Inertial fusion implosions



Nuclear Weapons



The equations of state of dense plasmas have many complications



$$U = U_{elec} + U_{ion} + U_{rad} \quad \text{Plasma internal energy}$$

$$P = P_{elec} + P_{ion} + P_{rad} \quad \text{Plasma pressure}$$

$$P_e = \bar{Z}n_i kT_e \quad \text{Ideal plasma}$$

or

$$\frac{\hbar^2}{5m_e} (3\pi^2)^{2/3} n_e^{5/3} \quad \text{Quantum degenerate plasma}$$

+ Coulomb effects

$$U_e = \frac{3}{2} \bar{Z}n_i kT_e + \sum_k n_k \left[\sum_{j=0}^k I_p^{(j)} \right]$$

ideal gas term

Energy in ionization

$$P_{ion} = n_i kT_i - \frac{2\pi}{3} n_i^2 \int_0^\infty \frac{\partial V(r)}{\partial r} g(r) r^3 dr$$

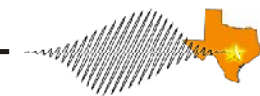
ideal gas term

Non-ideal correction where $g(r)$ = ion radial distribution function

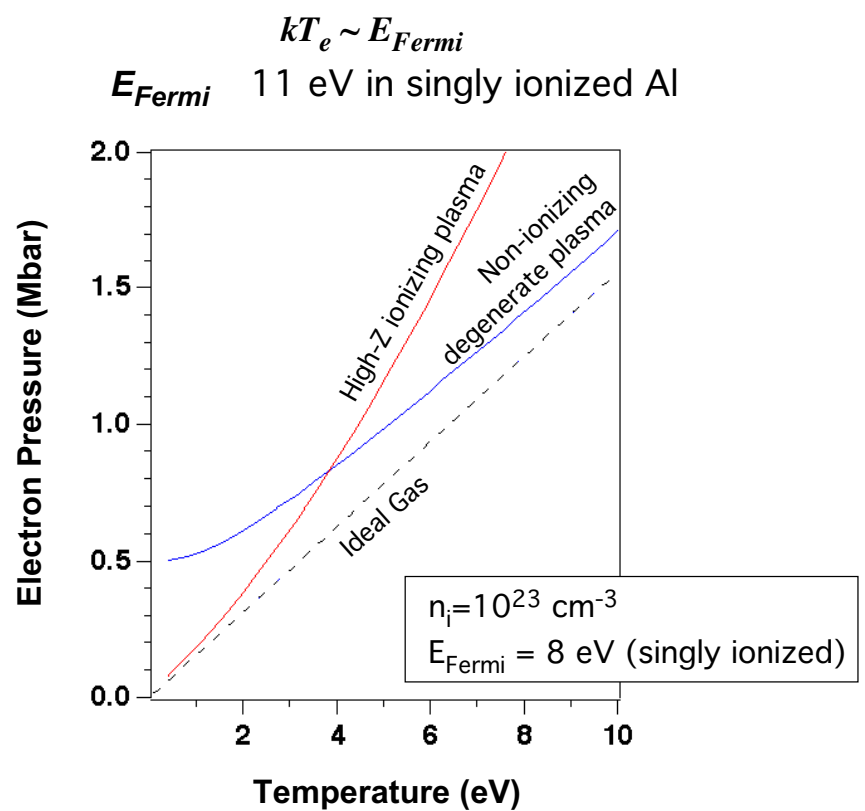
$$P_{rad} = \frac{\pi^2}{45} \frac{(kT_{rad})^4}{(\hbar c)^3}$$

Only important if optically thick: ie $\lambda_{hv} \Delta x_{plasma}$

Both quantum and Coulomb effects play an important role in the electron EOS

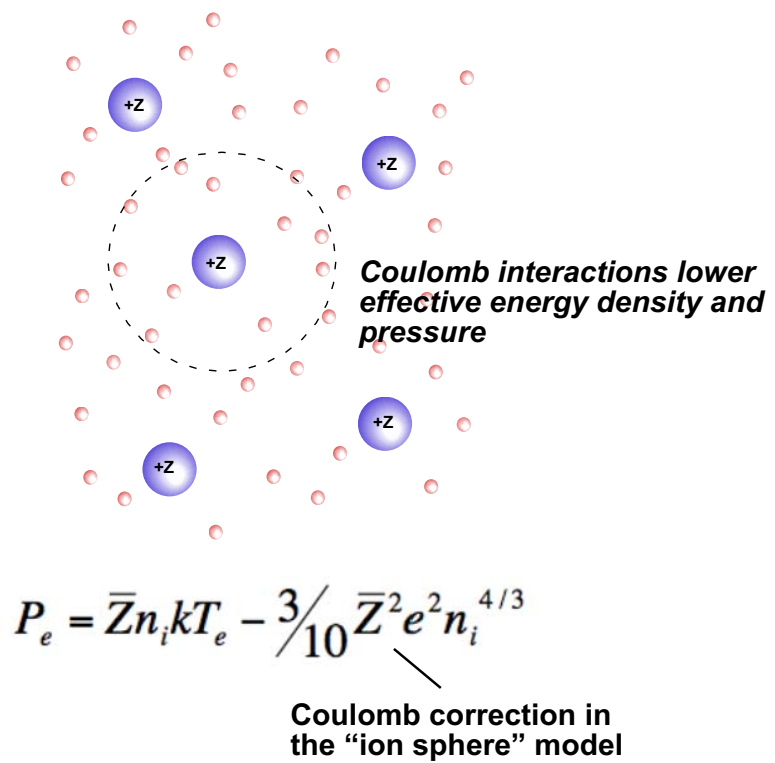


Quantum degeneracy effects:



Degeneracy effects ~ 20% when $kT_e \sim E_{Fermi}$

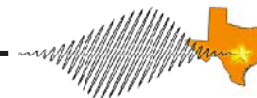
Coulomb effects:



Coulomb effects are a 50% correction with $n_i \sim 10^{23} \text{ cm}^{-3}$, $Z = 3$, and $kT = 50 \text{ eV}$

At solid density, Fermi energy is ~ 10 eV. Many HED plasmas have temperature in this vicinity, mandating a quantum mechanical treatment of the plasma

Ionization models do not converge in the HED plasma regime



Saha equilibrium equations for ion charge states

- Low to moderate density
- High temperature

$$\frac{n_e n_Z}{n_{Z-1}} = 2 \frac{W_Z(T)}{W_{Z-1}(T)} \left(\frac{m_e k T_e}{2\pi\hbar^2} \right)^{3/2} \exp \left[-\frac{I_p^{(Z-1)} - \Delta I_p^{(CL)}}{k T_e} \right] \quad n_e = \sum_{j=1}^{Z_{nuc}} n_j$$

“Average Atom” picture based on Thomas Fermi Model

- High density
- Low to moderate temperature

$$\frac{d^2\chi}{dr^2} = \frac{4}{3\pi\hbar^3} (2m_e e^2)^{3/2} \frac{Z^{1/2}}{r^{1/2}} \chi^{3/2}$$



These models are complicated by many other factors

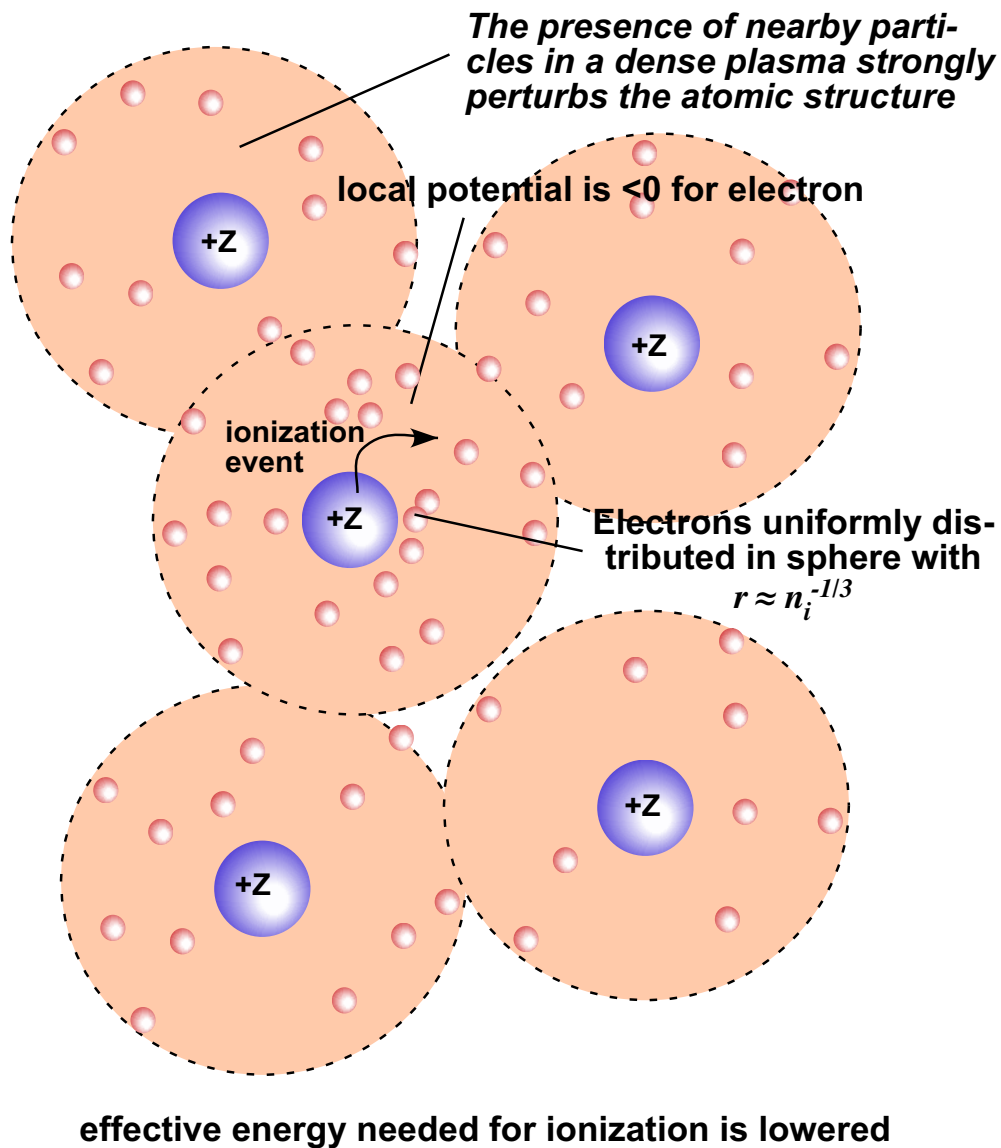
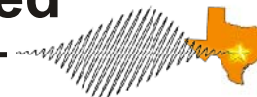
Co-existing constituents in a dense plasma:

- Ions
- Neutrals
- Negative ions
- Dimers
- Negatively charged dimers

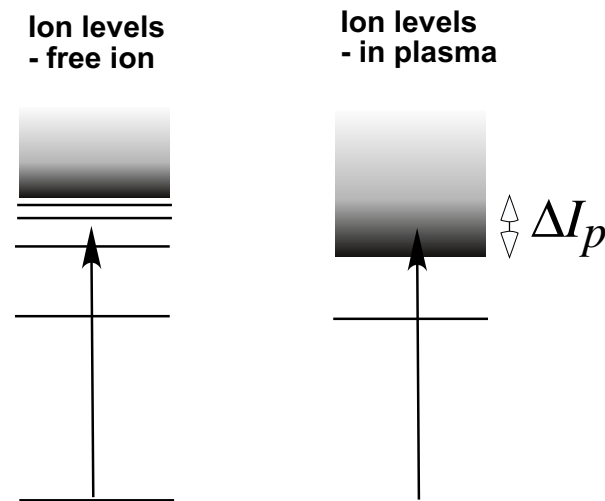
Electron affinity of Au: 2.3 eV

Bond strength of Al₂: ~ 5 eV

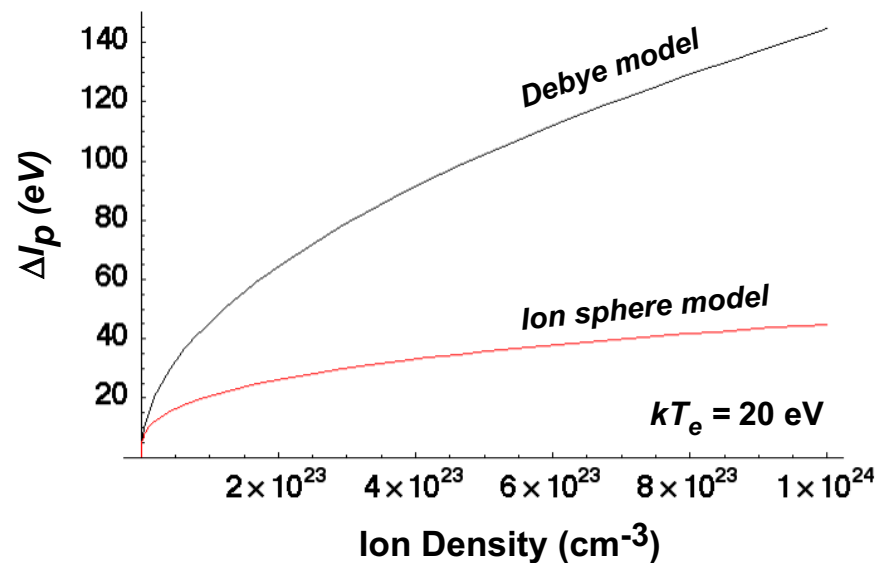
A significant question in dense plasmas is the extent to which the ionization potential of the plasma ions is altered



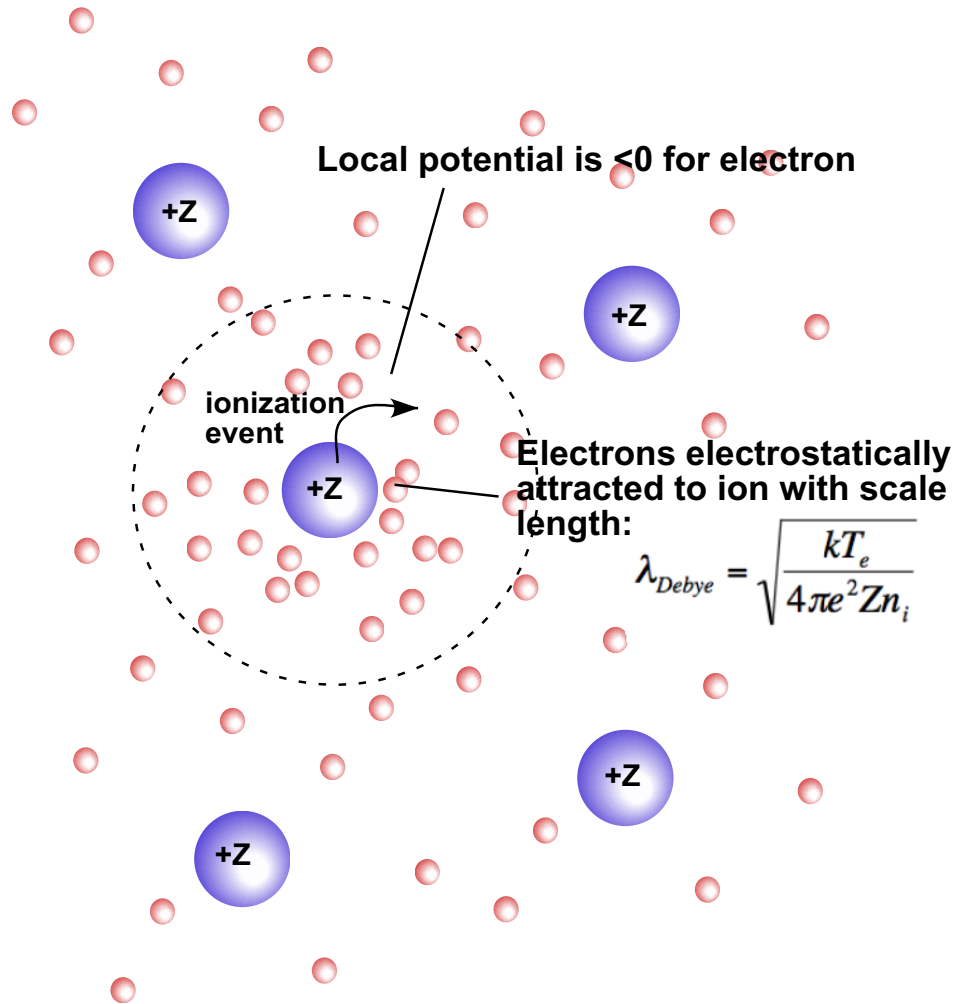
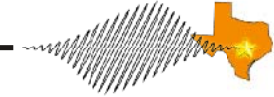
One significant effect is the lowering of the ionization potential: "Continuum lowering"



Continuum lowering predictions with a Saha model for ionization



The traditional method of calculating continuum lowering is to assume Debye shielding by the plasma electrons



Effective energy needed for ionization is lowered

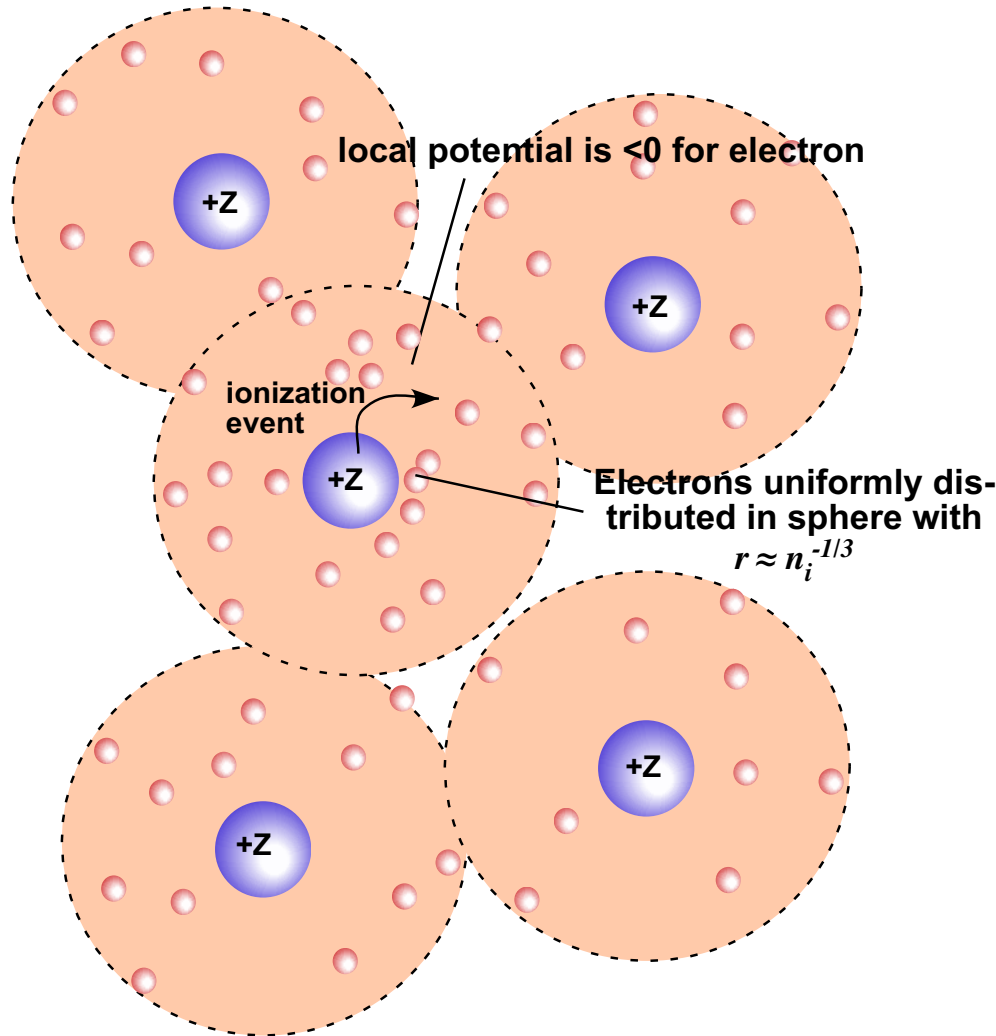
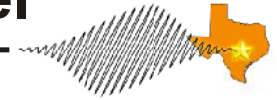
Debye model assumes WEAK coupling between electrons

- Linearizes Poisson's equation
- Calculate electrostatic energy of liberated electron to determine ionization potential lowering



$$\Delta I_p^{(Debye)} = 2Z^{3/2} e^3 \sqrt{\frac{\pi n_i}{kT_e}}$$

In strongly coupled plasma, the electrostatic continuum lowering can be estimated using the “ion sphere” model



In strongly coupled plasma Debye model does not work: use a simple “ion sphere model”

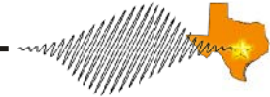
- Assume electrons are uniformly distributed within a sphere of radius $n_i^{-1/3}$
- Calculate electrostatic energy of liberated electron to determine ionization potential lowering



$$\Delta I_p^{(Z)} = \frac{9}{10} (2Z - 1) e^2 n_i^{1/3}$$

effective energy needed for ionization is lowered

Different continuum lowering models yield very different predictions in the strongly coupled regime



Continuum lowering model predictions:

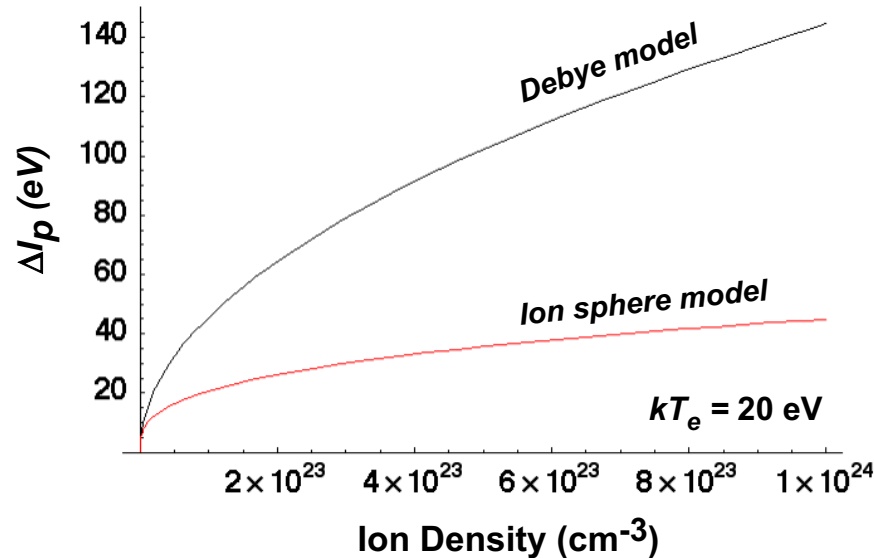
$$n_i = 2 \times 10^{23} \text{ cm}^{-3}$$

$$kT_e = 10 \text{ eV}$$

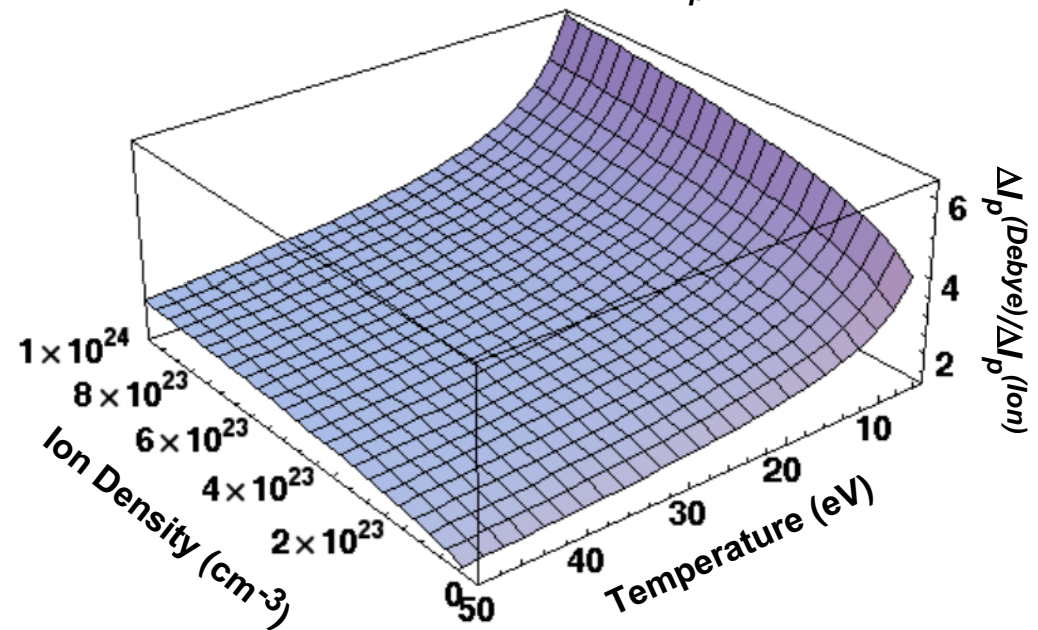
$$Z = 3$$

Quantum model	1.2 eV
Ion Sphere model	38 eV
Debye Model	140 eV

Continuum lowering predictions with a Saha model for ionization

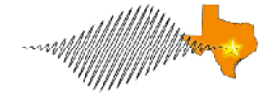


Ratio of Debye and Ion Sphere predictions for ΔI_p



We believe that the ion sphere model is most appropriate for the cold dense plasmas produced by XUV irradiation of clusters

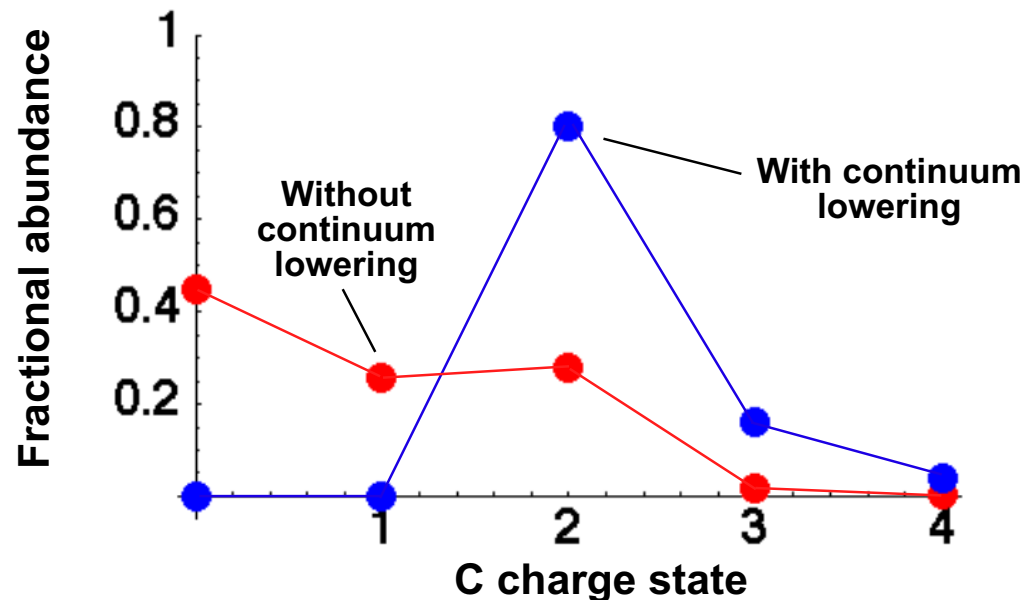
A Saha model of ionization in solid density carbon plasma illustrates the dramatic impact of continuum lowering



Saha equilibrium equations

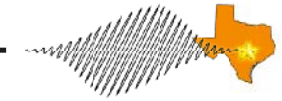
$$\frac{n_e n_Z}{n_{Z-1}} = 2 \frac{W_Z(T)}{W_{Z-1}(T)} \left(\frac{m_e k T_e}{2\pi\hbar^2} \right)^{3/2} \exp \left[-\frac{I_p^{(Z-1)} - \Delta I_p^{(CL)}}{k T_e} \right] \quad n_e = \sum_{j=1}^{Z_{nuc}} n_j$$

Charge distribution in a solid density Carbon plasma with 15 eV electron temperature

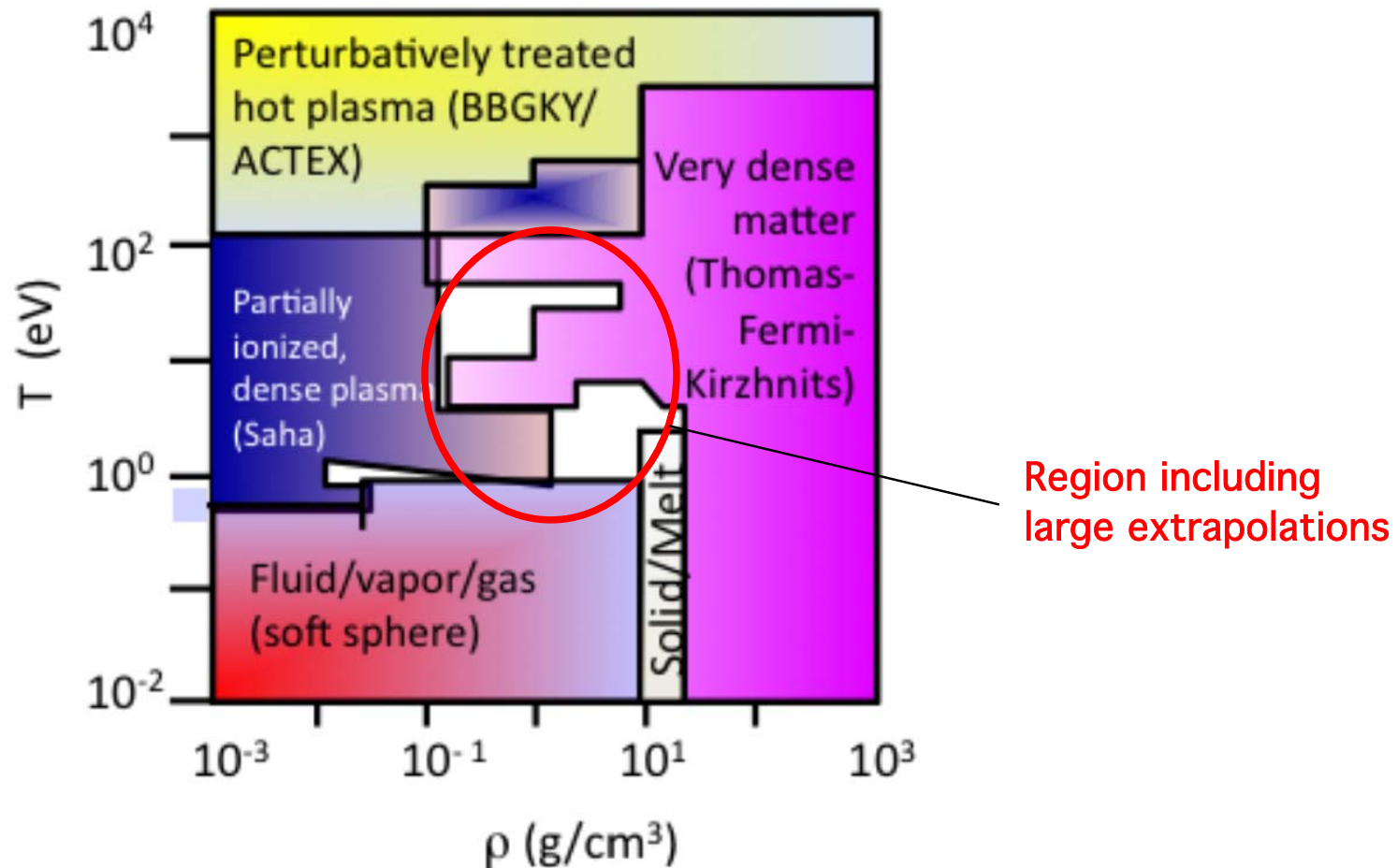


Saha collisional equilibrium implies about twice the electron density in a carbon plasma with continuum lowering

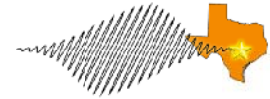
The common theoretical practice is to piece together many different models in the WDM regime



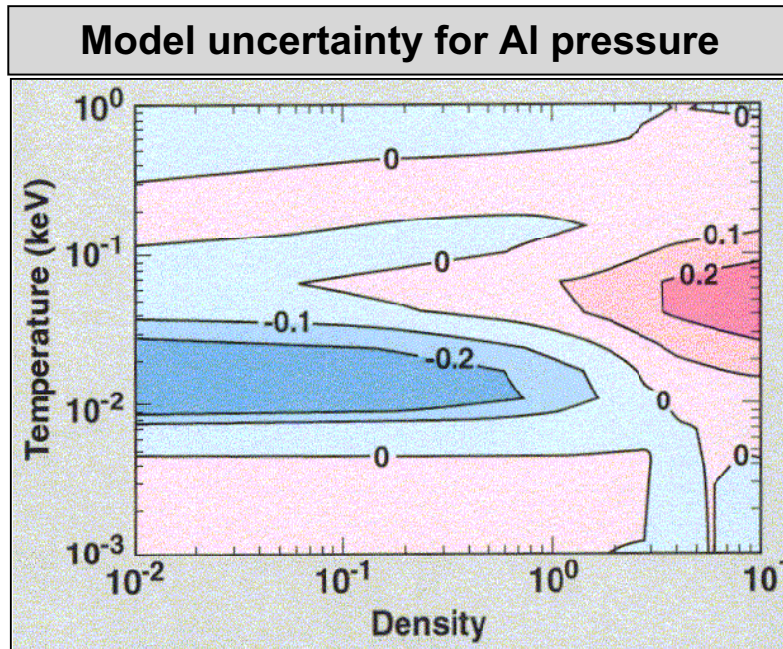
ρ - t diagram (copper): the range of applicability for the best theories in each region, including intricate corrections



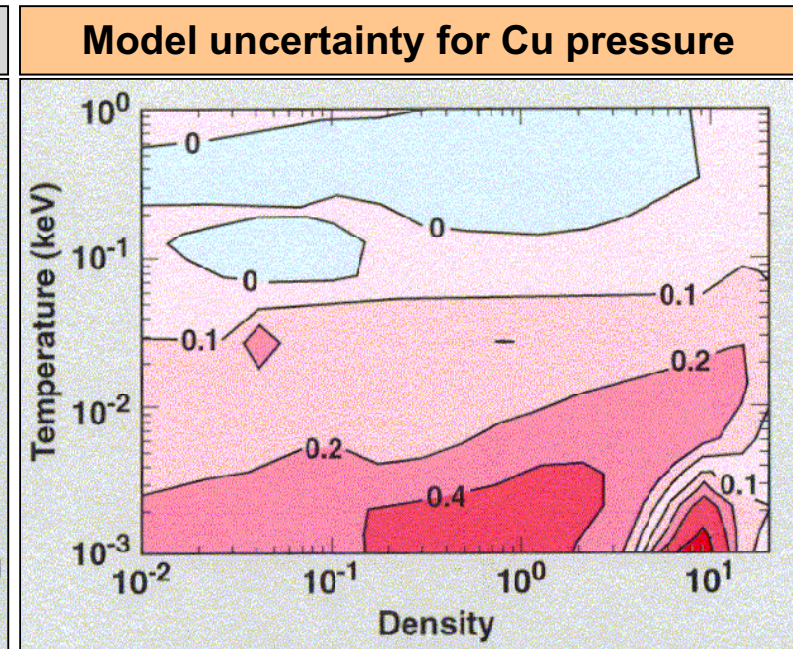
In the warm/hot dense matter regime sizeable errors exist in the equation of state



Contours of fractional difference in pressure predicted by different models



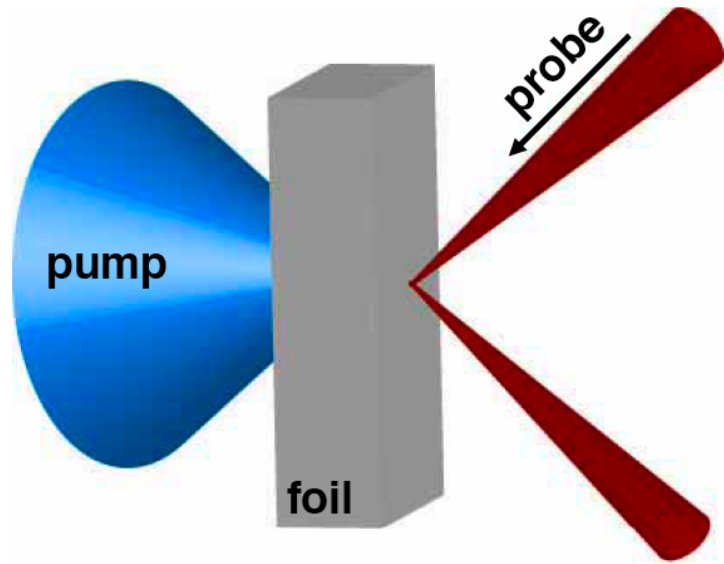
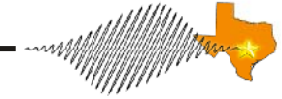
- Simple atomic physics
- Although most studied, differences of more than 20% in calculated pressure values can be found in the regime for hot expanded states;



- Complex atomic physics - d-shell electrons
- Large model differences in the WDM region
- Measurements required for guidance

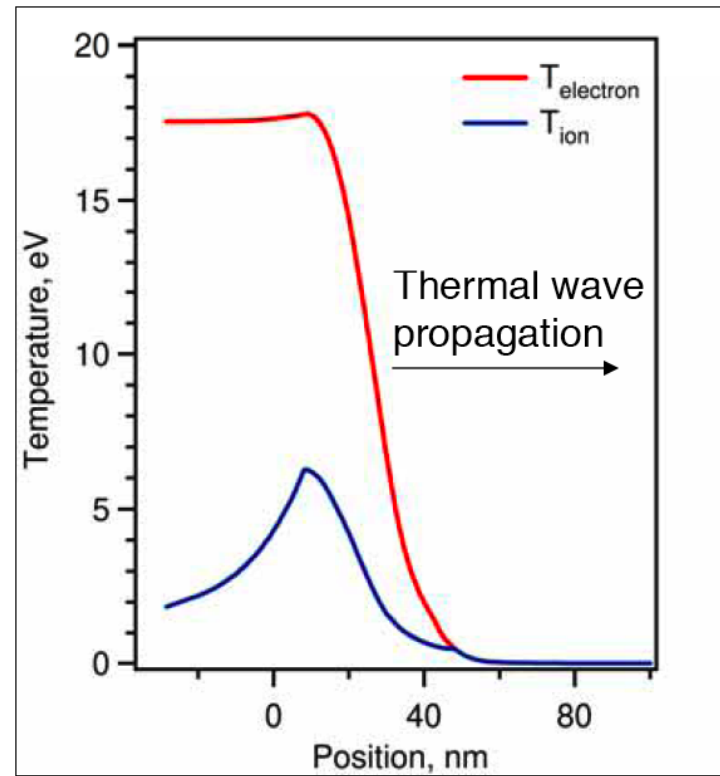
Implementation of atomic physics in this (ρ , T) regime is very challenging

We use direct laser heating of thin foils to study plasmas with temperatures of 1-10 eV

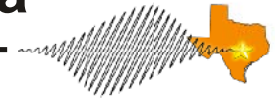


Electron (red) and ion (blue) temperature distributions in Al foil 500fs after it was heated with 60 fs pulse at $2 \cdot 10^{14}$ W/cm².

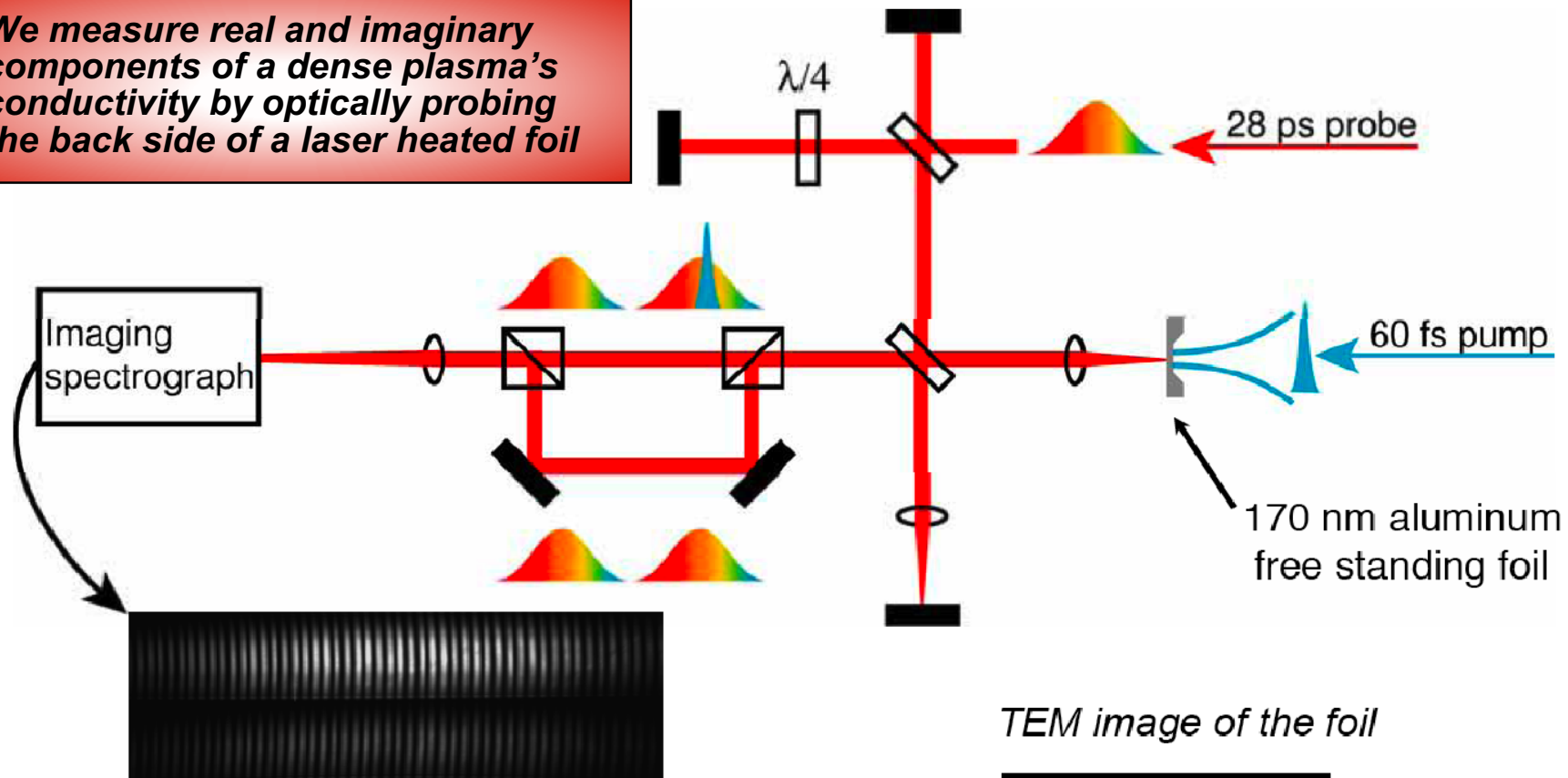
Optically probing the back surface of the foil will allow us to investigate non-equilibrium phenomena due to direct femtosecond laser heating.



Using chirped probe pulses, we can measure the time evolution of the optical properties of a laser-heated plasma

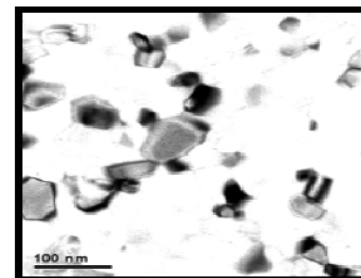


We measure real and imaginary components of a dense plasma's conductivity by optically probing the back side of a laser heated foil



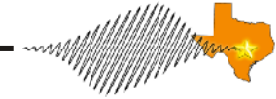
Two sets of probe pulses were split from the pump pulse to perform the entire experiment with a single shot.

TEM image of the foil

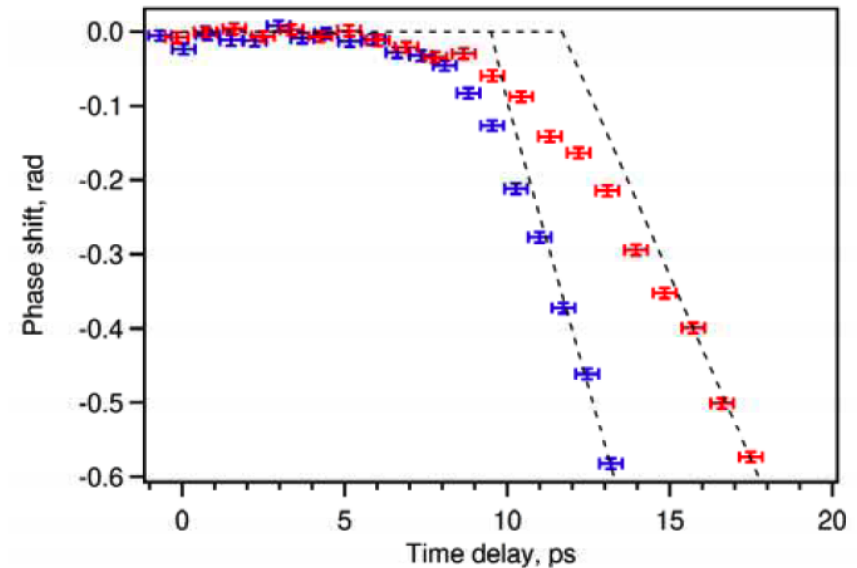
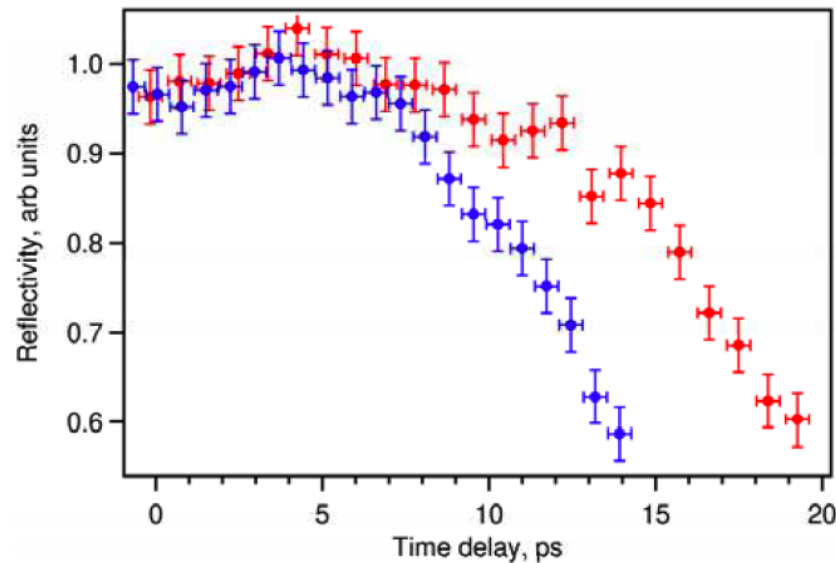


- FCC structure
- Polycrystalline
- grain size ~40nm

We have measured the optical properties of dense Al plasma heated with a 40 fs pulse



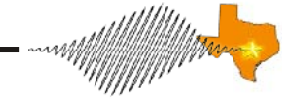
Back surface reflectivity and phase shift of 170 nm foil irradiated with $2.2 \cdot 10^{14} \text{W/cm}^2$ (blue) and $1.6 \cdot 10^{14} \text{W/cm}^2$ (red) intensities.



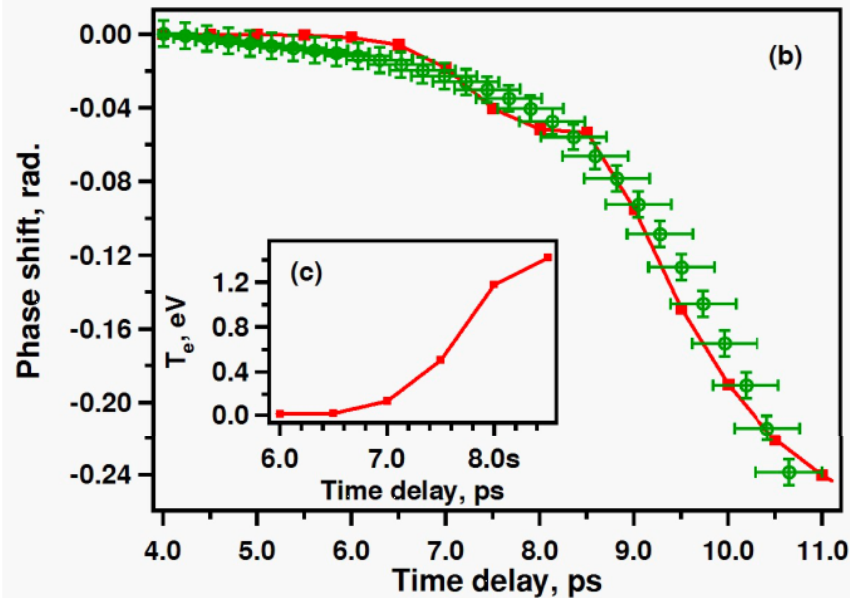
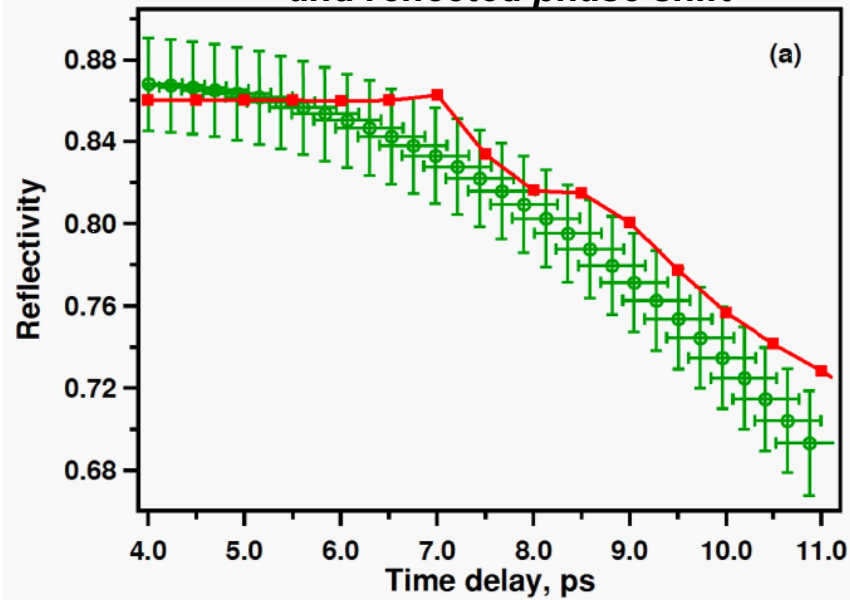
- For the first few ps the returned probe signal stays unchanged.
- 6ps later the heat wave reaches the back surface of target, electron temperature rises.
- >10 ps Shock wave reaches the back surface. Phase shift changes are dominated by the particle motion as material expands

So, between 6 and 10 ps we have a heated back surface with a sharp interface to vacuum

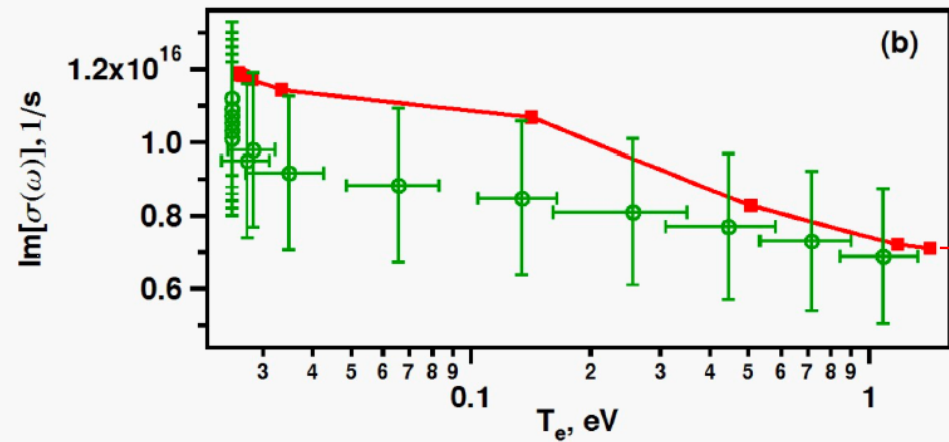
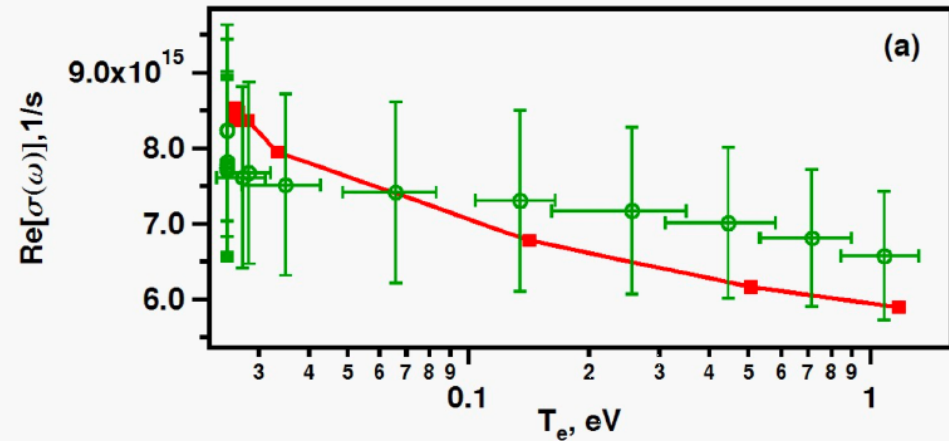
Our measurements are roughly consistent with a well known dense plasma conductivity model



Measured time dependence of reflectivity and reflected phase shift



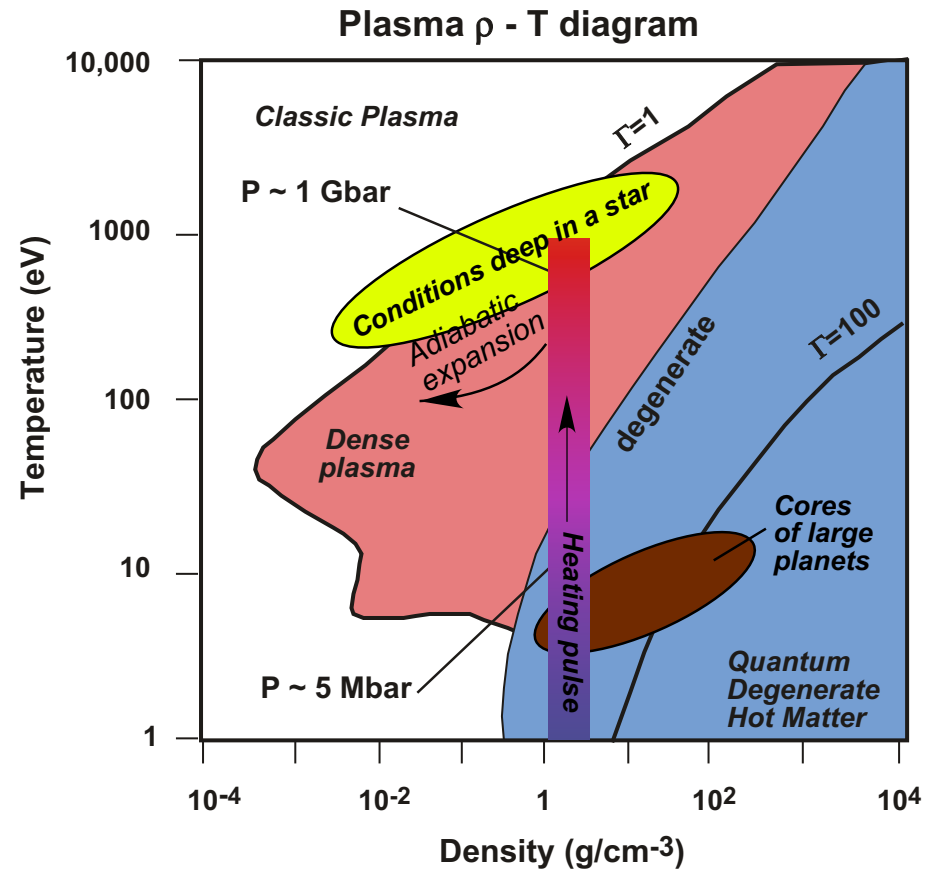
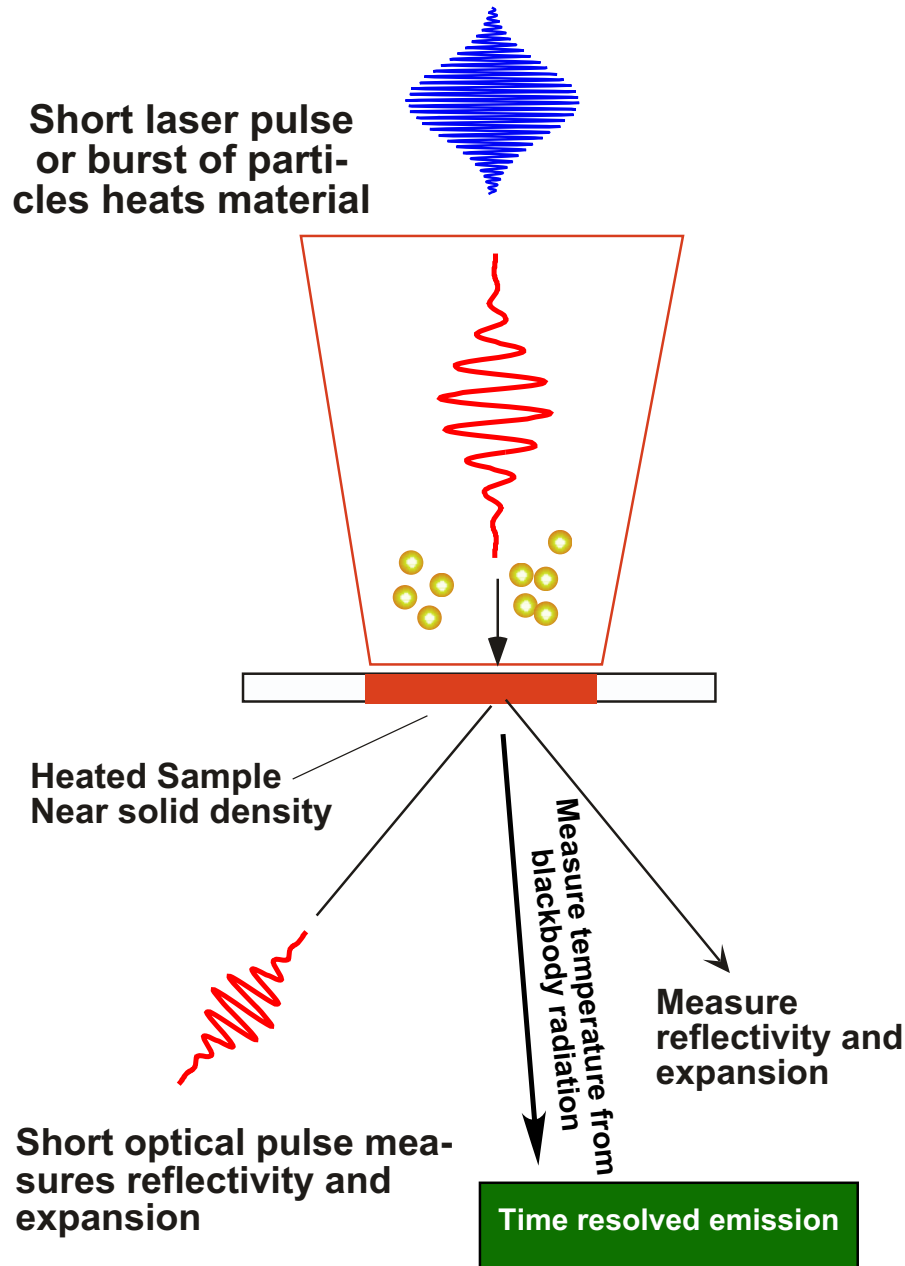
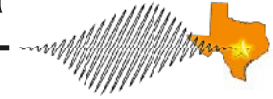
Derived real and imaginary conductivity



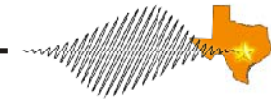
Predictions of the LEE & More model

Y. T. Lee and R. M. More, *Phys. Fluids* 27, 1273 (1984).

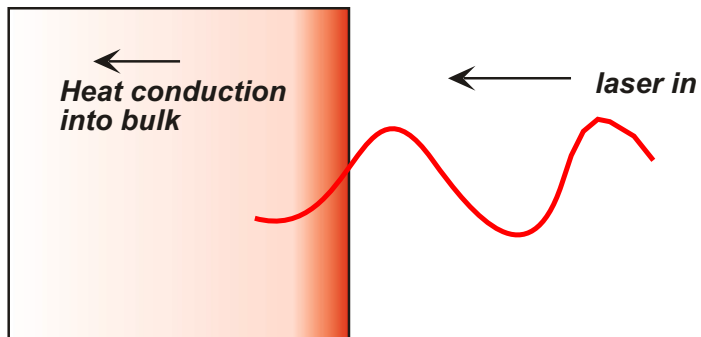
Isochoric heating can be combined with optical and x-ray probes to derive information about a hot dense plasma



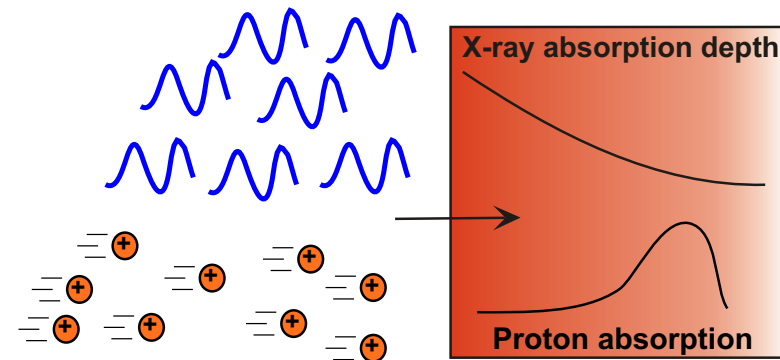
Short pulse laser produced radiation can be used to heat isochorically bulk matter



Optical radiation heats only over one skin depth ~10-100 nm



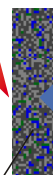
Protons (1 - 10 MeV) deposit energy within the bulk of a target (10-100 μm)



Petawatt laser in



Secondary target



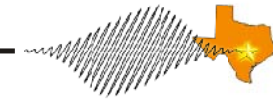
optical (or x-ray) probe
• interferometry
• reflectivity
• x-ray diffraction

This slab target producing x-rays, electrons or protons (Al, Ti, Cu etc.)

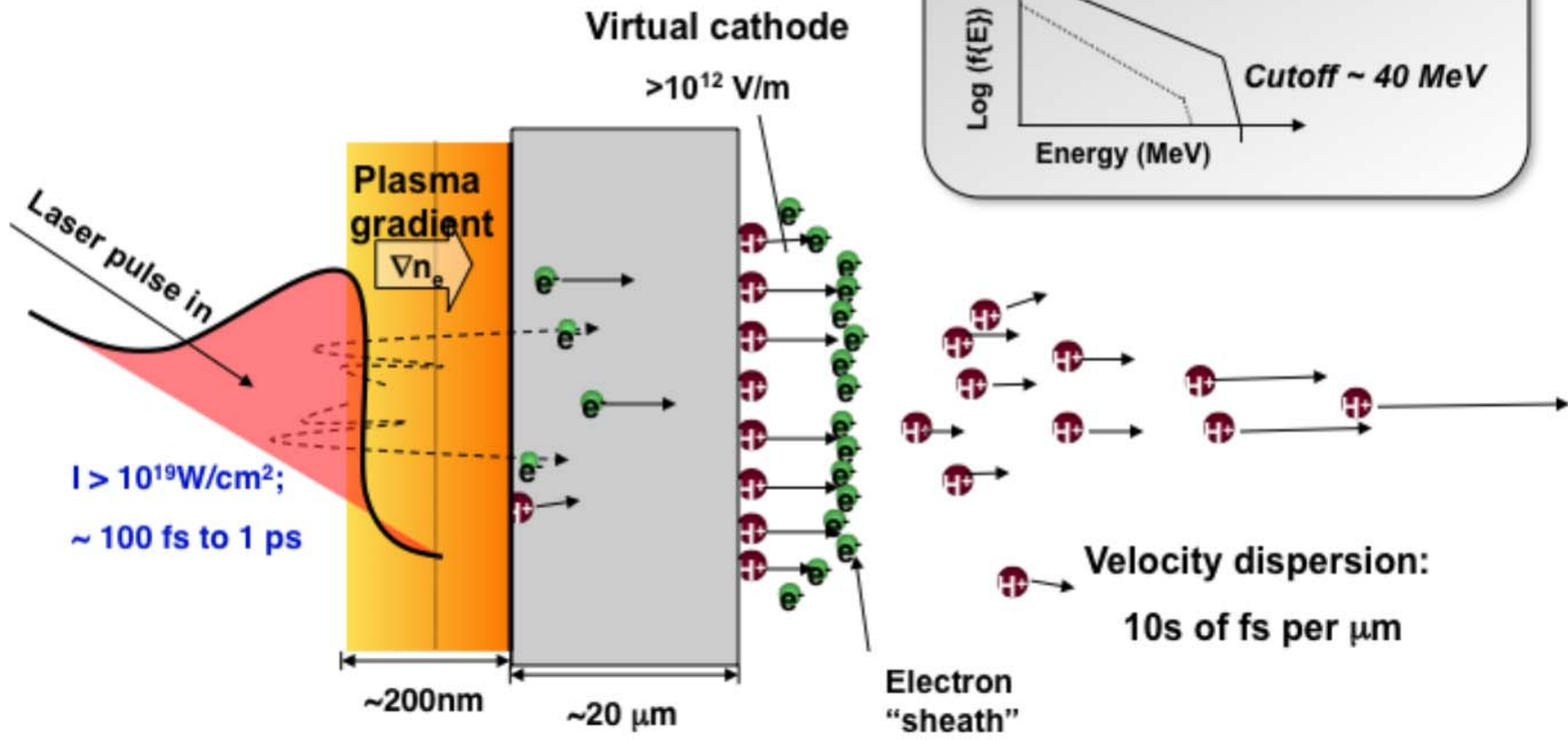
K- α x-rays, protons etc. from laser plasma

Primary target

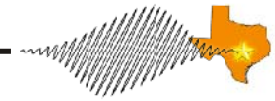
With a petawatt laser, very intense, energetic pulses of protons can be produced



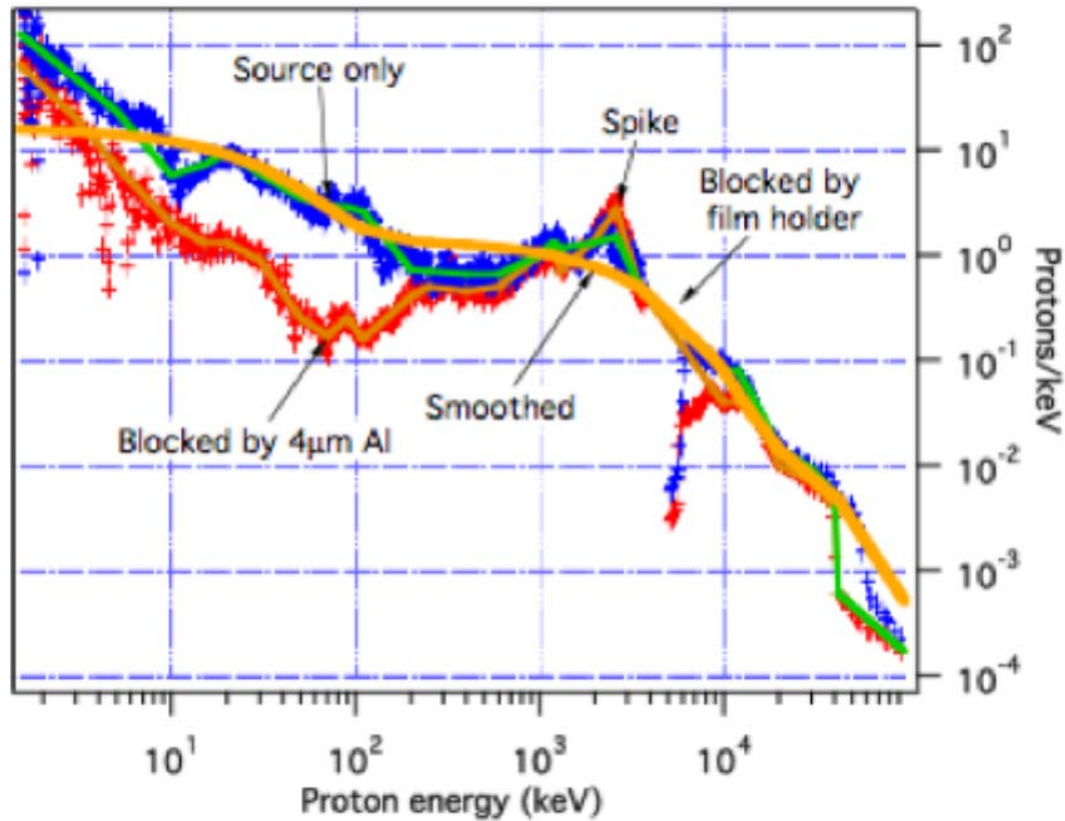
Protons are present on metal foil surfaces
in the form of H₂O and hydrocarbons
(moderate vacuum $\sim 10^{-5}$ Torr)



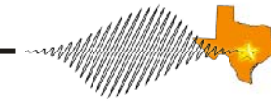
Proton spectra from PW irradiation of solids are typically broad, stretching to a cut-off of many MeV



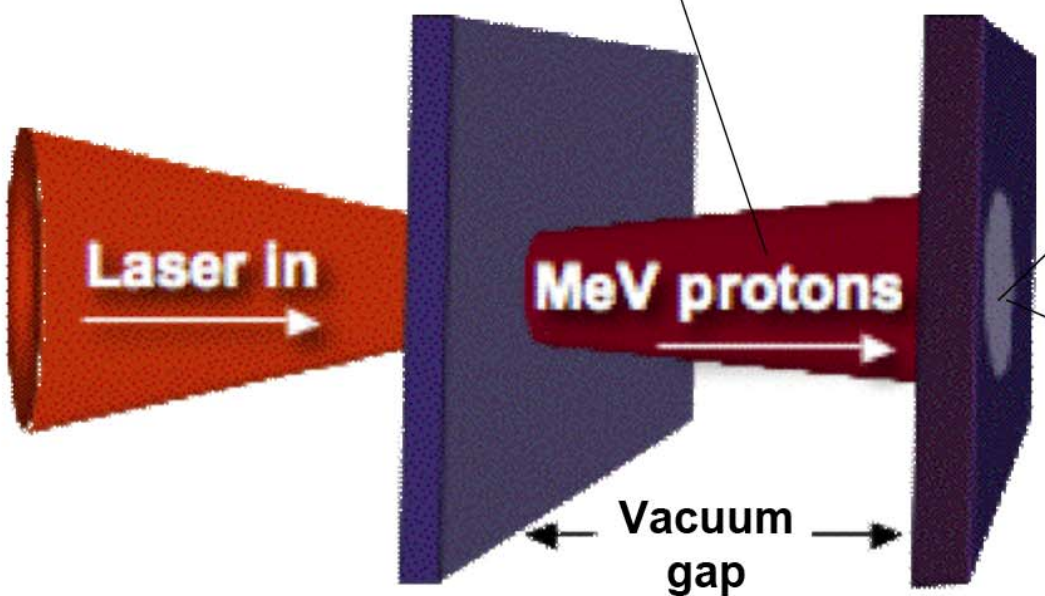
Proton spectrum from Titan irradiation of a slab target



A petawatt-class laser can generate multi-joule pulses of protons to heat a secondary solid target



- Directional
- Efficiency ~1% from laser energy
- Heats sample several μm deep
- Not mono-energetic \rightarrow velocity dispersion



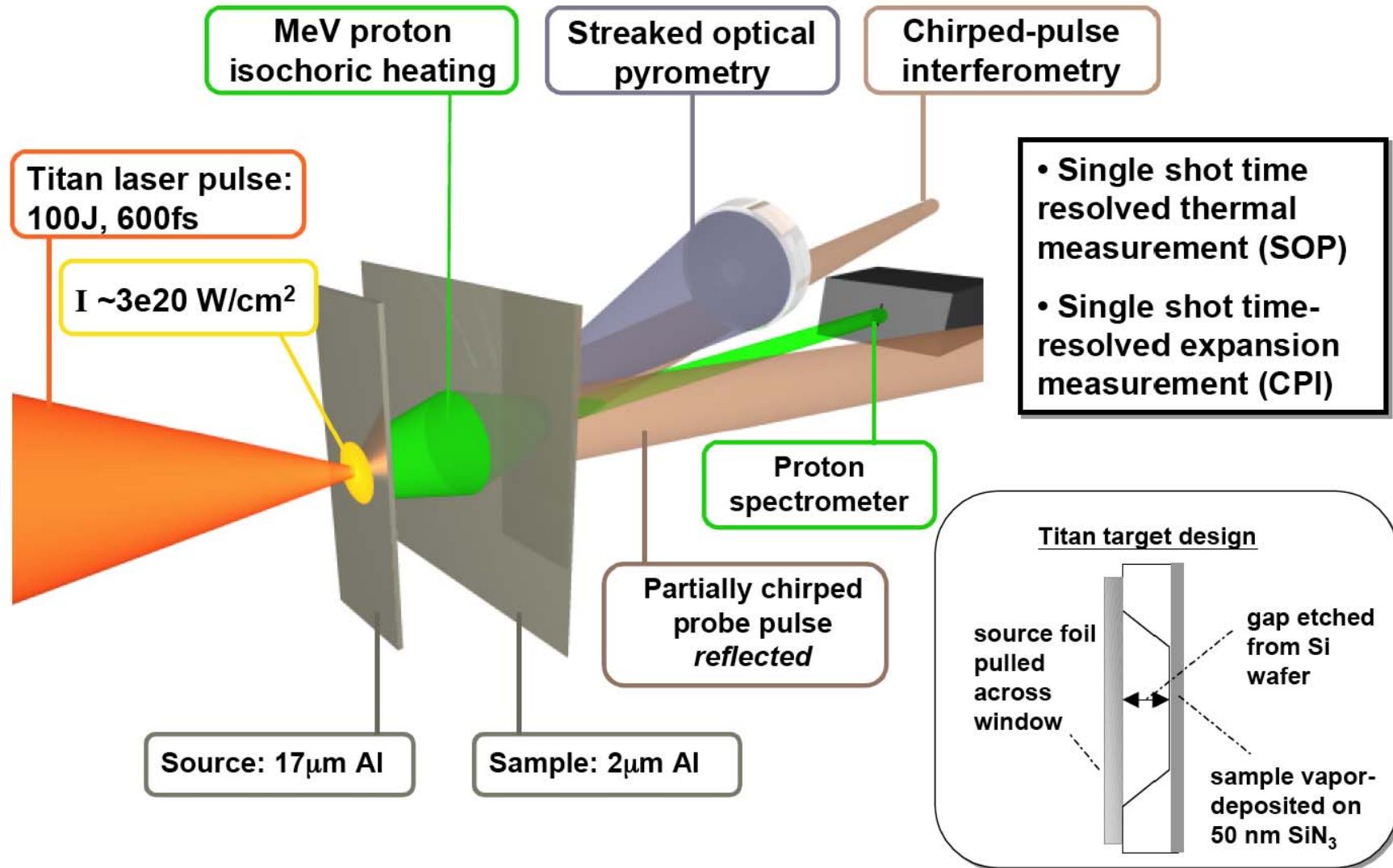
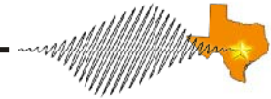
$P > 4 \text{ Mbar}$
 \Rightarrow Rapid expansion into vacuum
 $\Rightarrow v > 10^6 \text{ cm/s}$

$T > 10\text{eV}$
 \Rightarrow Blackbody emission through visible and UV
 \Rightarrow Few-ps timescale

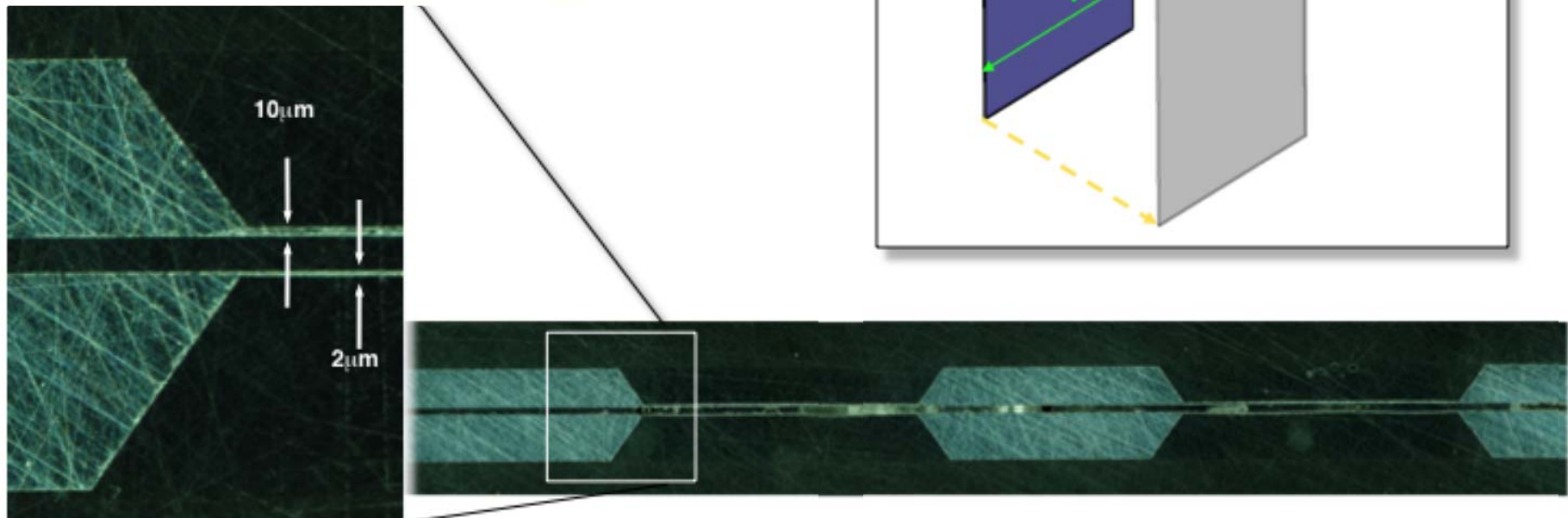
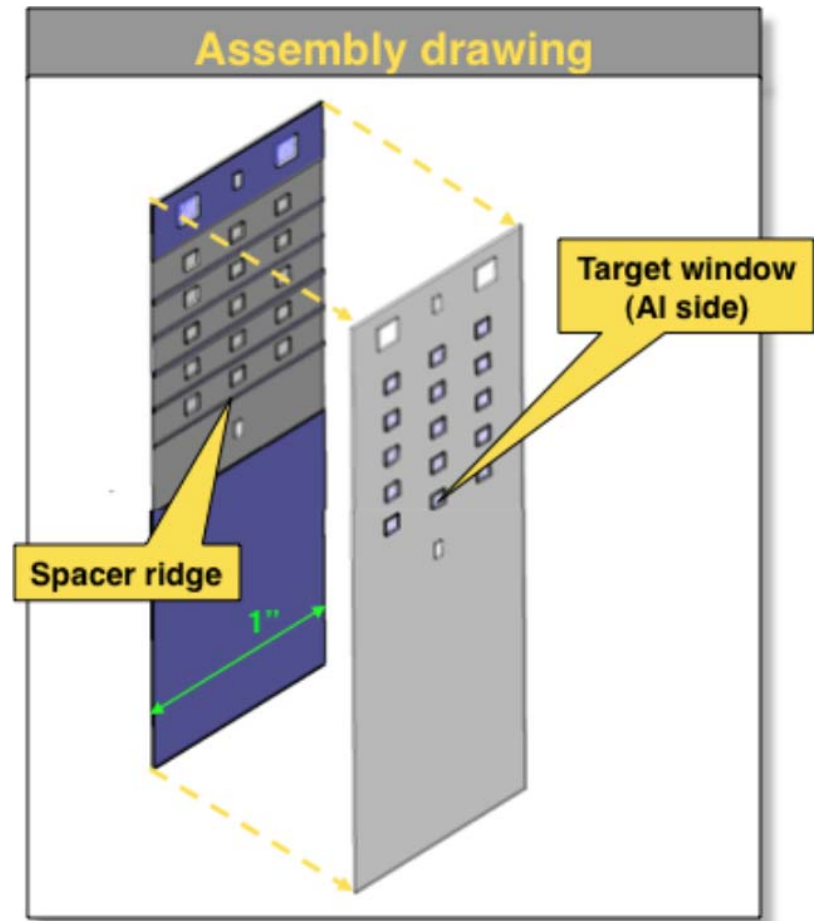
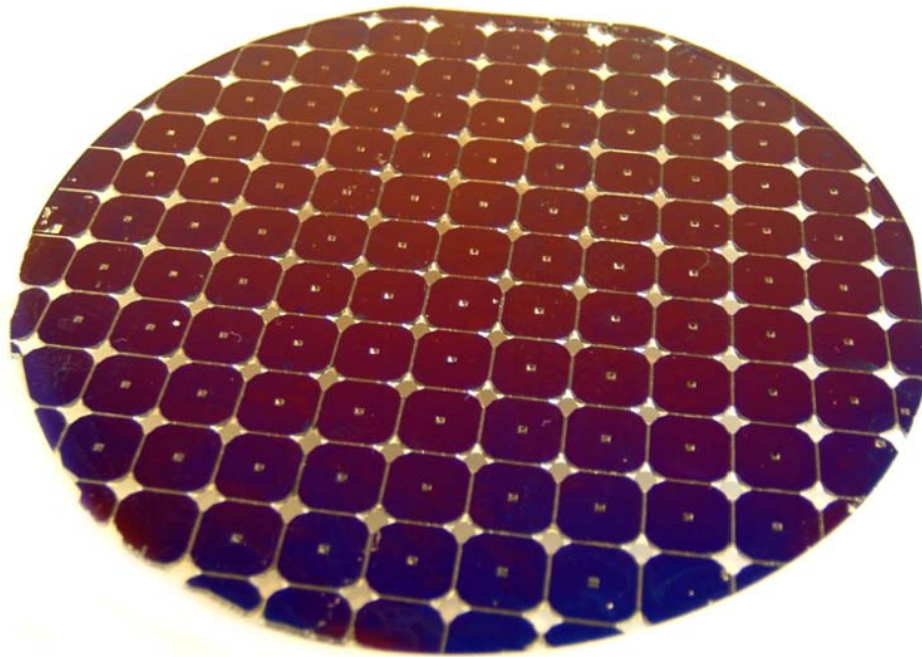
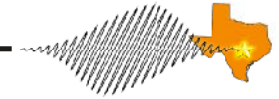
SOURCE

SAMPLE

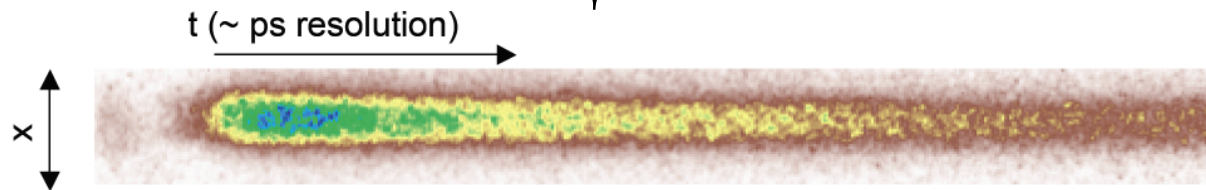
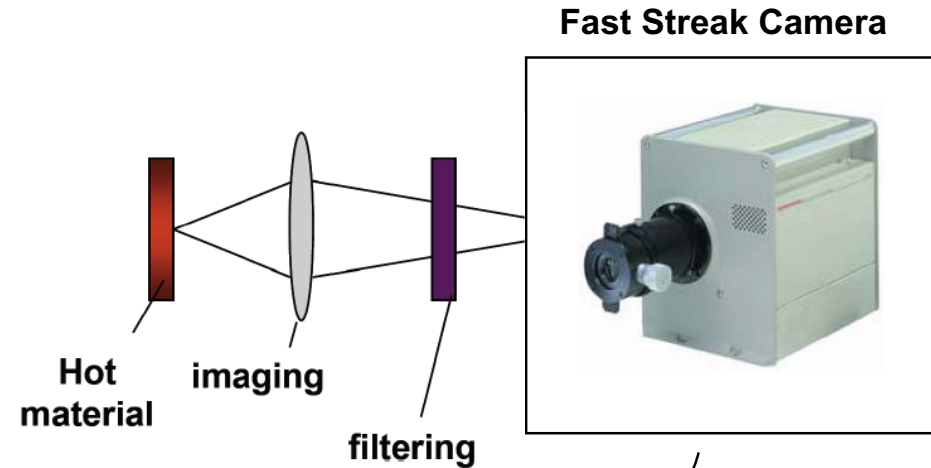
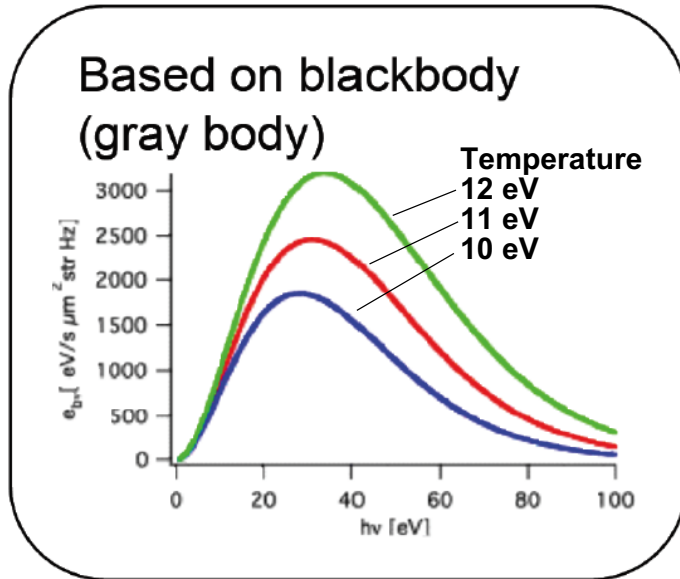
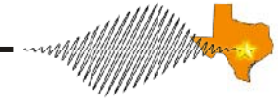
We have demonstrated proton heating using the LLNL 200 TW Titan laser



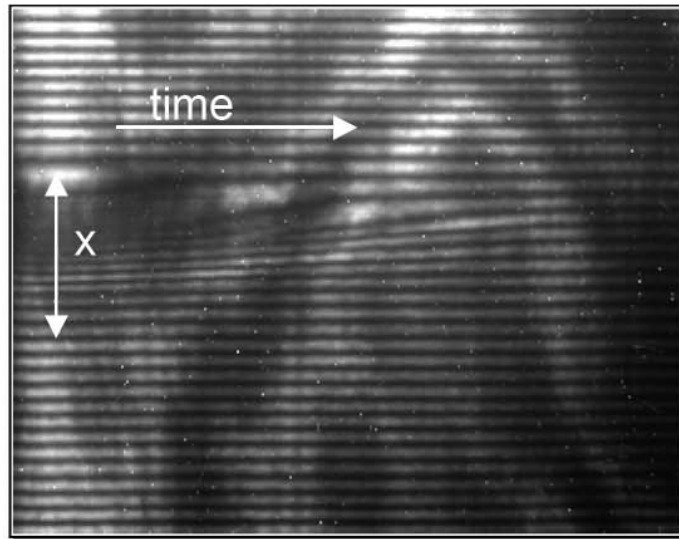
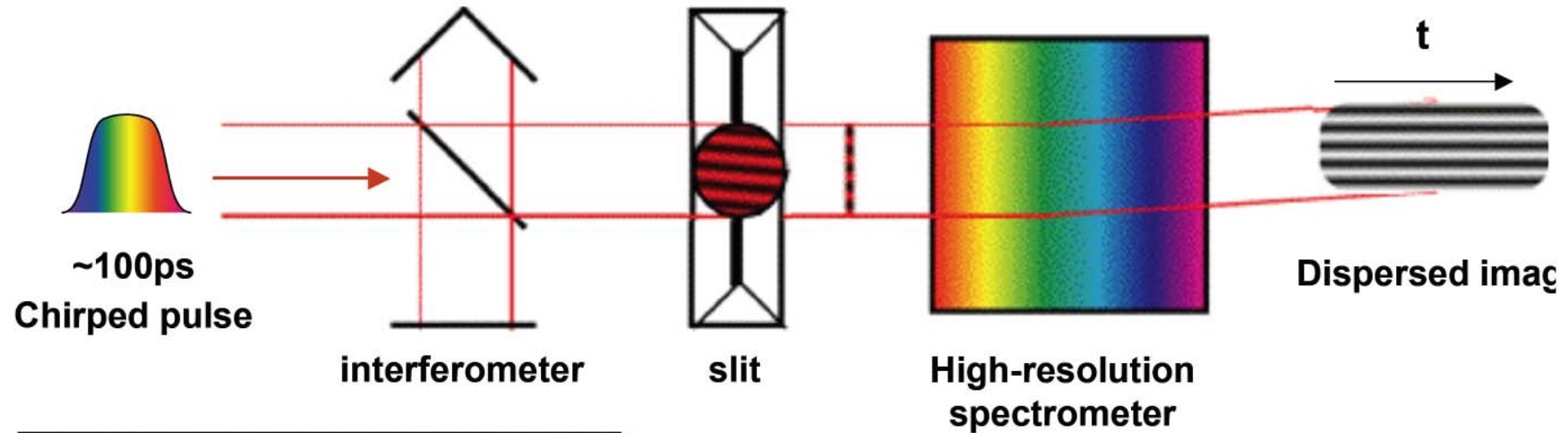
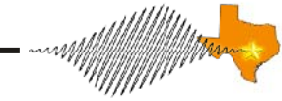
Multi-layer targets for proton isochoric heating experiments can be fabricated in silicon wafers



The plasma's temperature is independently measured with a streaked optical pyrometer



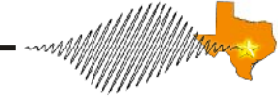
We measure the expansion rate of the heated plasma with chirped pulse interferometry



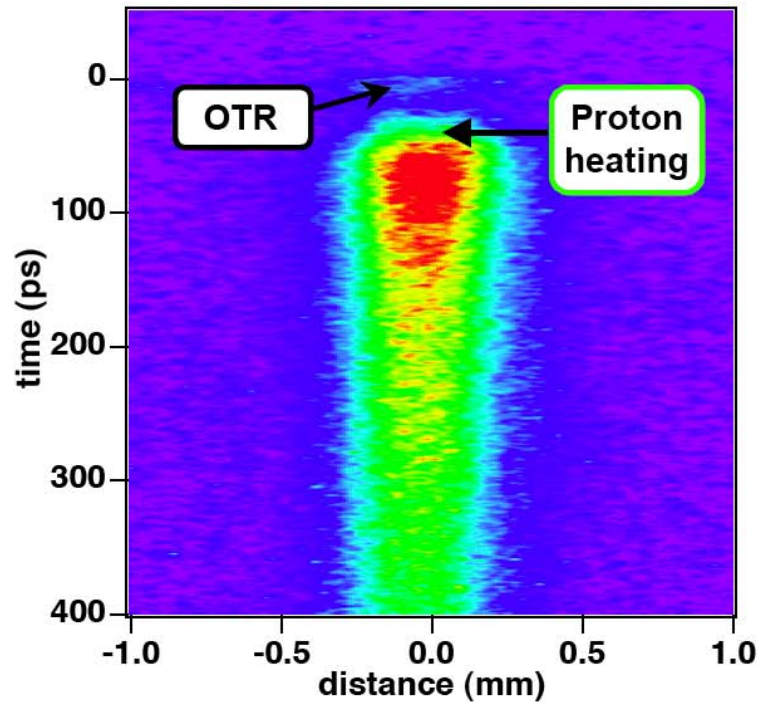
- **Chirped: Spectrum \rightarrow Time**
- **Bending of fringes \rightarrow changing in time**
- **$\Delta t_{\text{resolved}} \sim \Delta t_{\text{unchirped}}$ (post process)**

J. P. Geindre, P. Audebert, S. Rebibo, and J. C. Gauthier. Single-shot spectral interferometry with chirped pulses. *Optics Letters*, 2001.

The time history of the temperature and expansion of the heated Al slab was measured on every shot

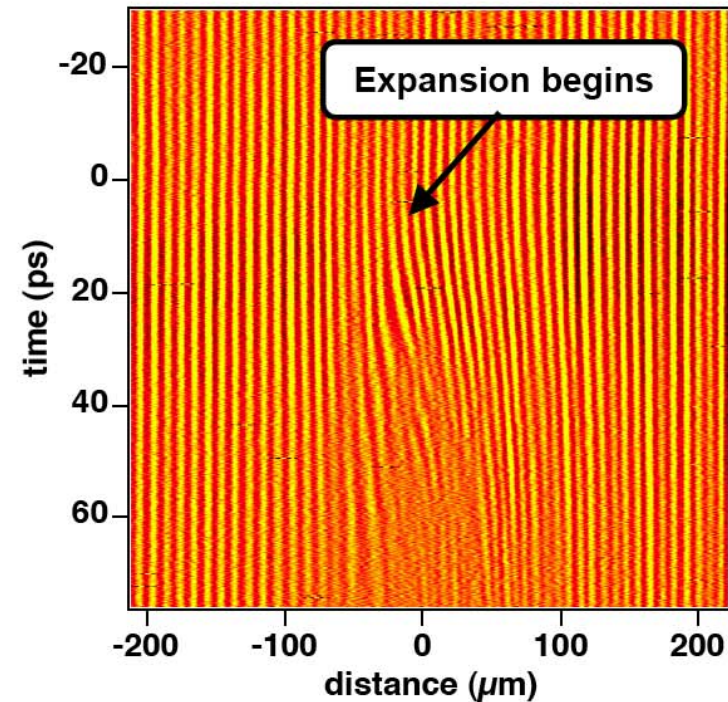


SOP: Time-resolved temperature



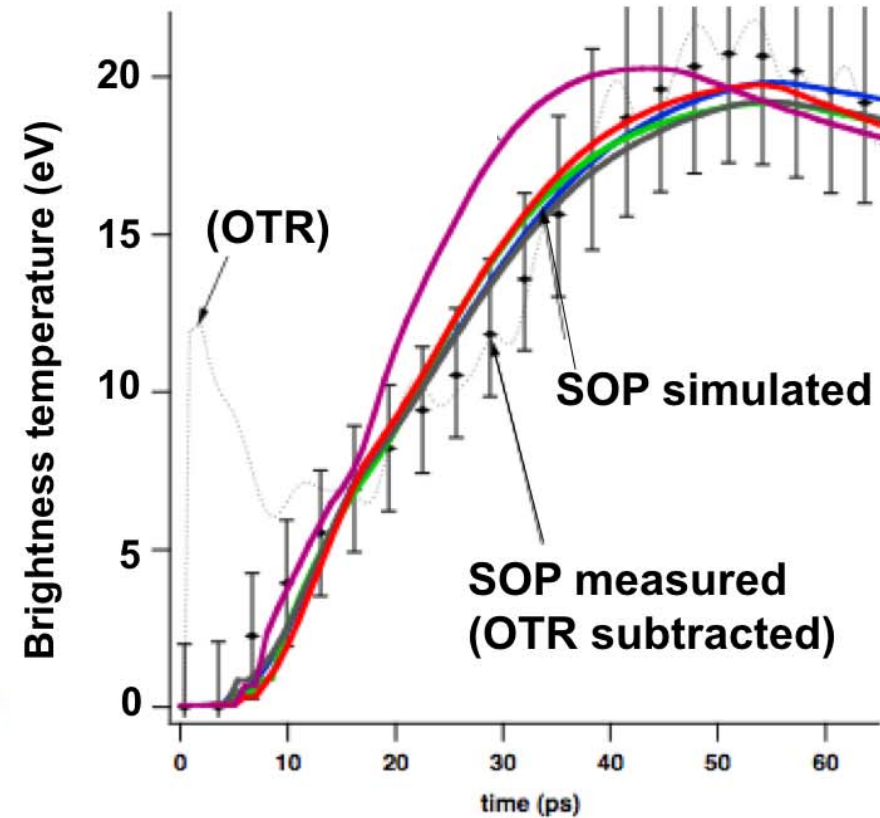
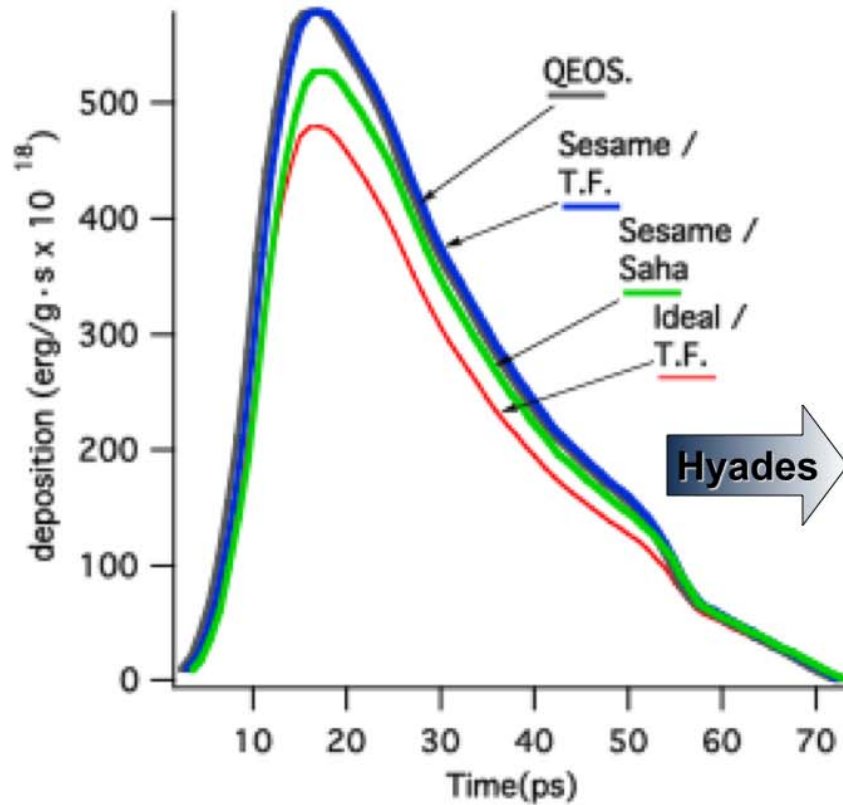
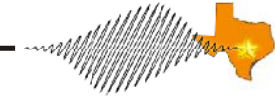
- Peak temperature ~ 25 eV
- Optical transition radiation signal at t_0

CPI: Time-resolved expansion

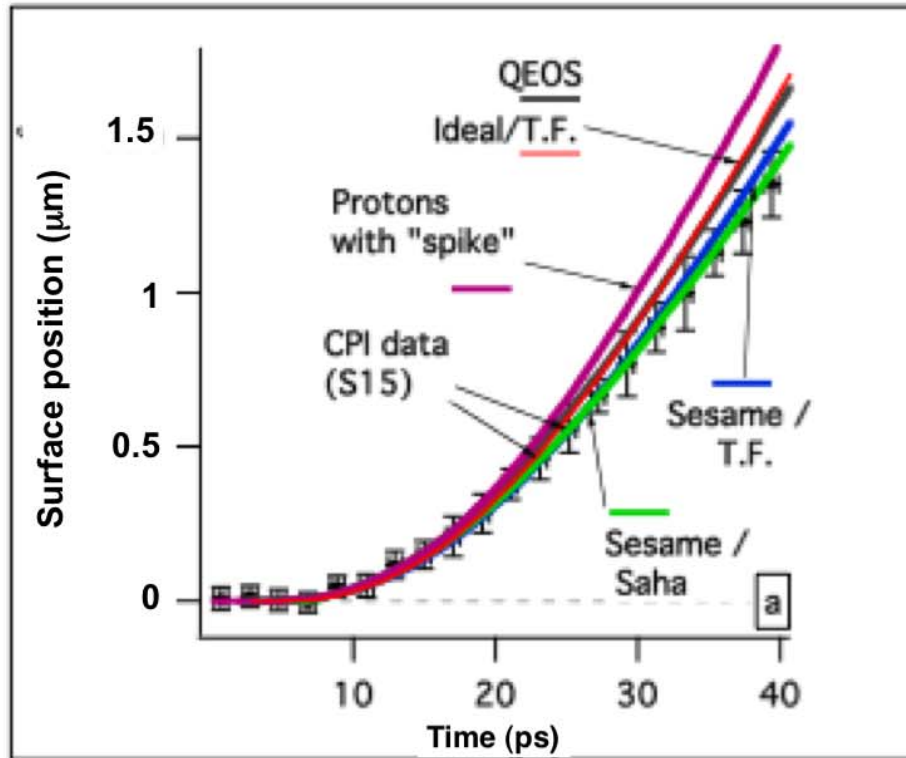
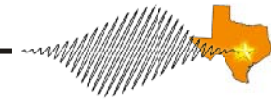


- Fourier analysis of bending fringes
→ phase shift → expansion in time

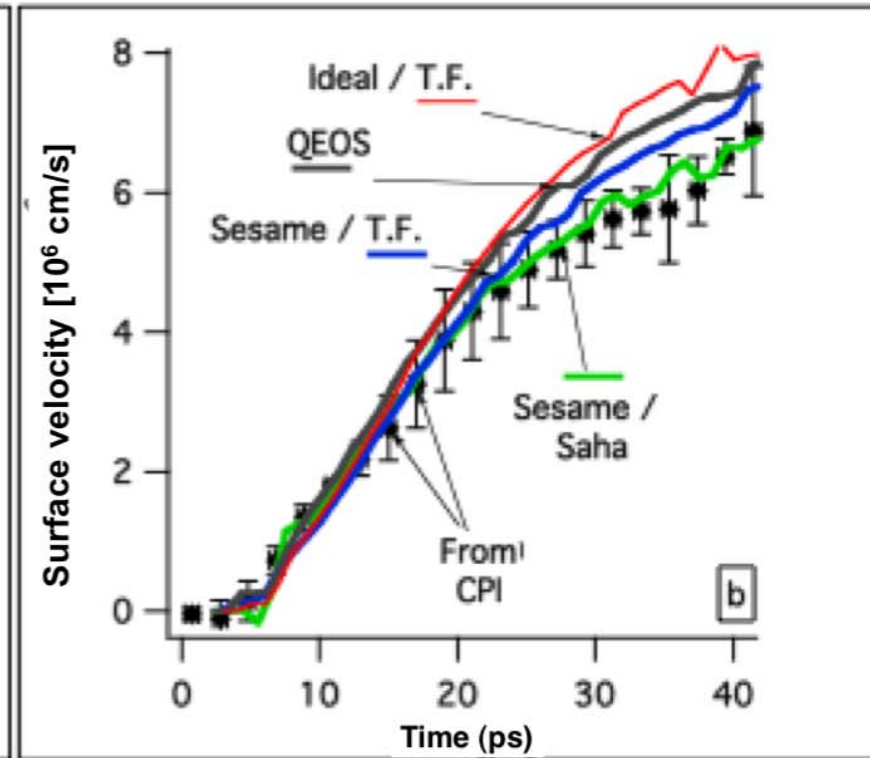
Time-resolved measurement of black-body emission indicated that we heated the solid Al to 20 eV



Our proton-heated Al had an EOS which was consistent with the most commonly used SESAME table



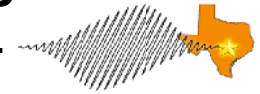
Sesame / Saha fits expansion curve within 4%



Sesame / Saha fits velocity curve within 10%

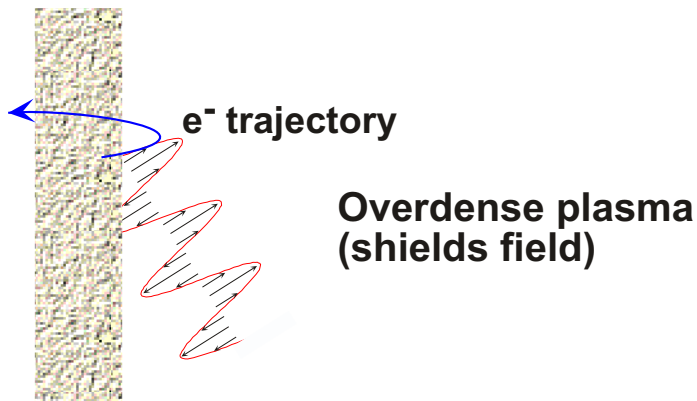
This measurement was in solid density aluminum at a maximum temperature of 20 eV

“Rescattering” of laser driven electrons at the surface of a sharp plasma gradient can produce pulses of fast electrons



Scattering at the conducting surface breaks the adiabaticity of the laser oscillation

→ **“Brunel absorption”**



1) Oscillating laser field accelerates electrons

2) Electrons fly into target

Solid Target

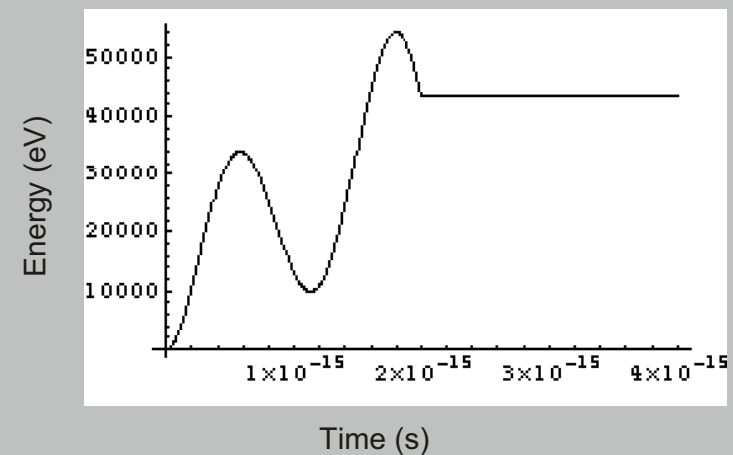
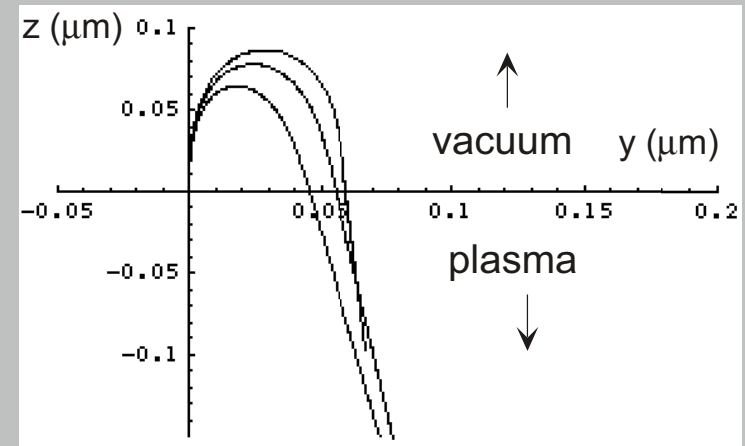
4) Electrons are directed normal to target surface

Intense ultrafast pulse

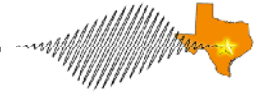
Hot dense plasma

3) Electron bunches are driven into the target spaced by one wavelength

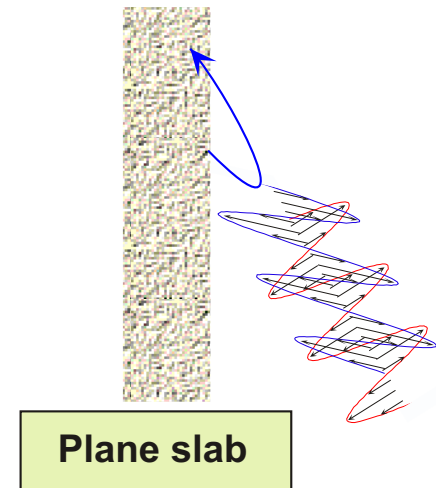
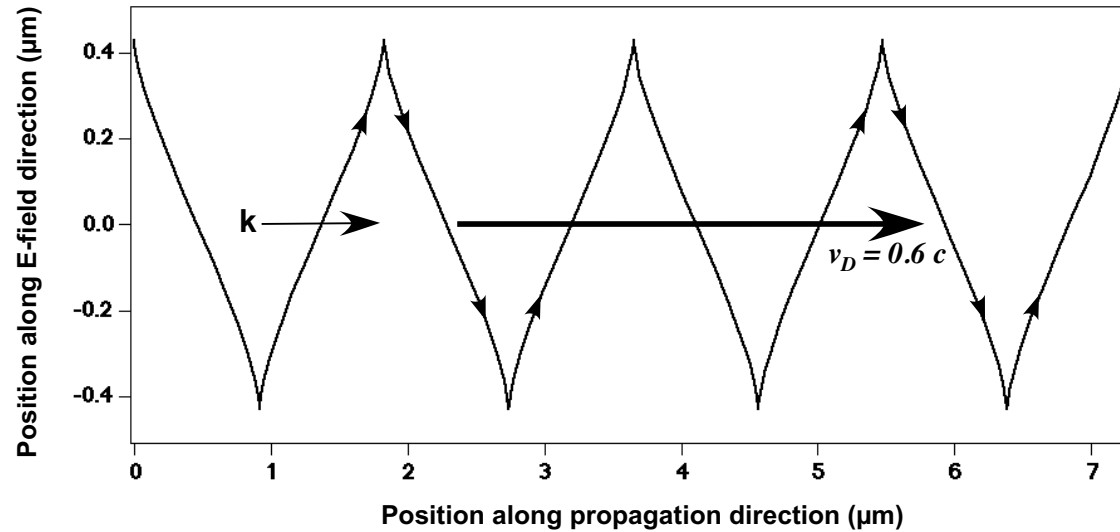
Simulated e⁻ trajectories and energy in relativistic field at plasma surface
 $U_p = 50 \text{ keV} (5 \times 10^{17} \text{ W/cm}^2)$



At relativistic intensity, the laser's magnetic field can also accelerate electrons at a sharp surface



Electron trajectory with $\lambda = 1 \mu\text{m}$ and $I = 10^{19} \text{ W/cm}^2$, ($a_0 = 2.7$ and $\gamma_{osc} = 2.1$)



1) Oscillating electric and magnetic fields accelerate electrons

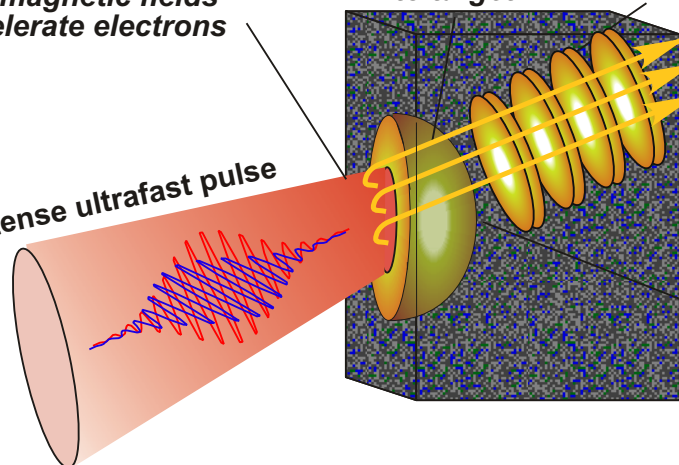
2) Electrons fly into target

Solid Target

4) Electrons are directed along laser wave vector

3) Electron bunches are driven into the target spaced by one half a wavelength

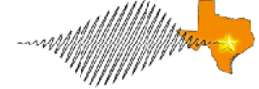
Intense ultrafast pulse



“ $j \times B$ heating”

$$T_{hot} \approx U_p^{(rel)} = (\gamma_{osc} - 1) m_e c^2$$

Transport of laser accelerated electrons on a solid target can be diagnosed by imaging their transition radiation



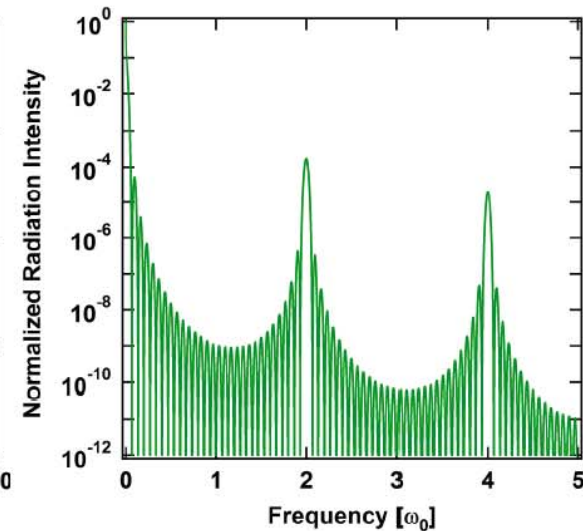
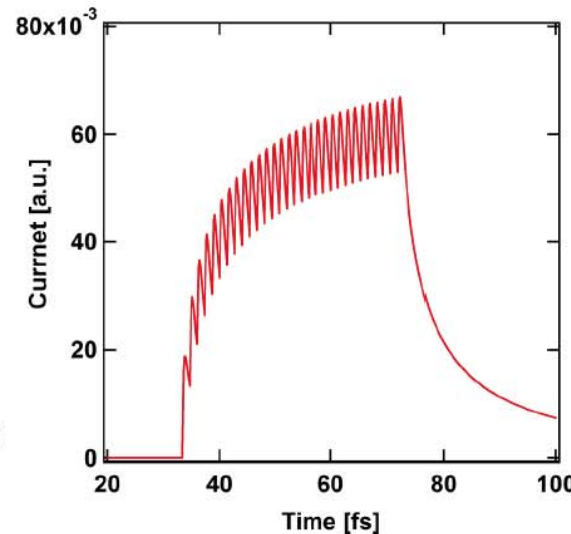
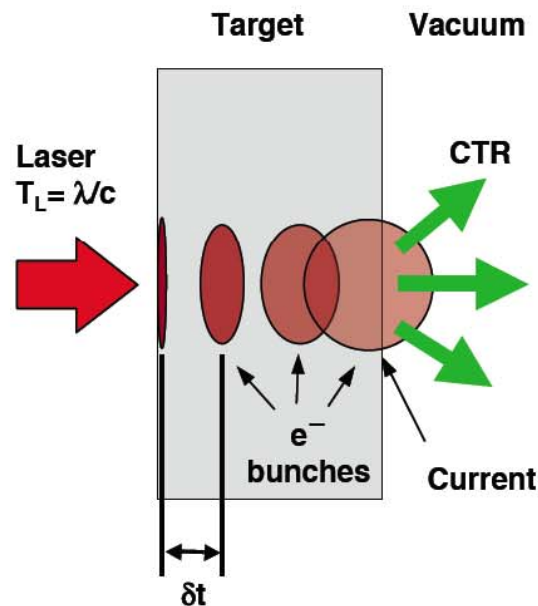
Ballistic transport model

Electrons injected into the target have a relativistic Maxwellian velocity distribution

Current at target rear side generated by 30 e^- bunches in 40 fs

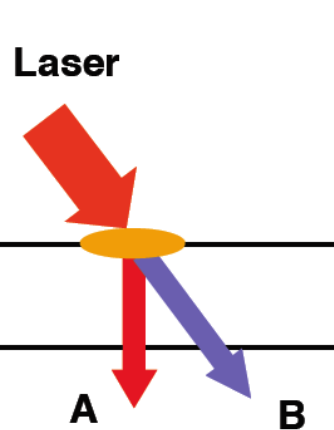
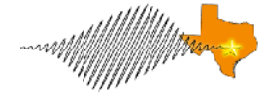
Radiation spectrum is given by Fourier transform of current

$$I_{CTR} = \eta(\omega)P^2 |j(\omega)|^2 \frac{\sin^2(M\omega\delta T/2)}{\sin^2(\omega\delta T/2)}$$

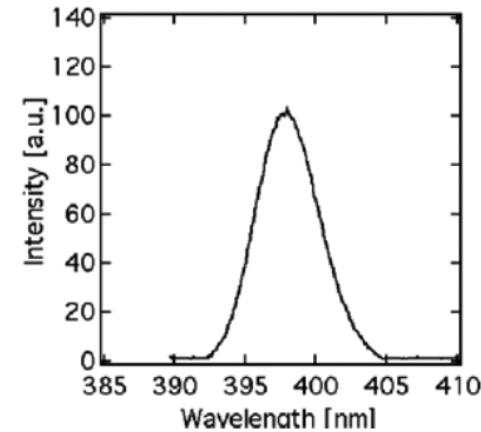
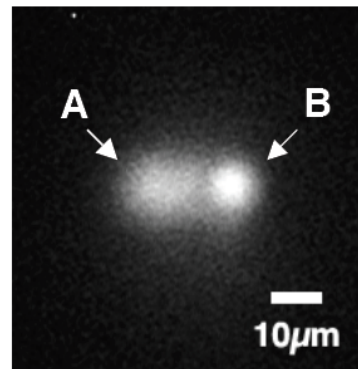


$$T_e = 1 \text{ MeV}, \delta t = 1.33 \text{ fs}, d = 10 \mu\text{m}$$

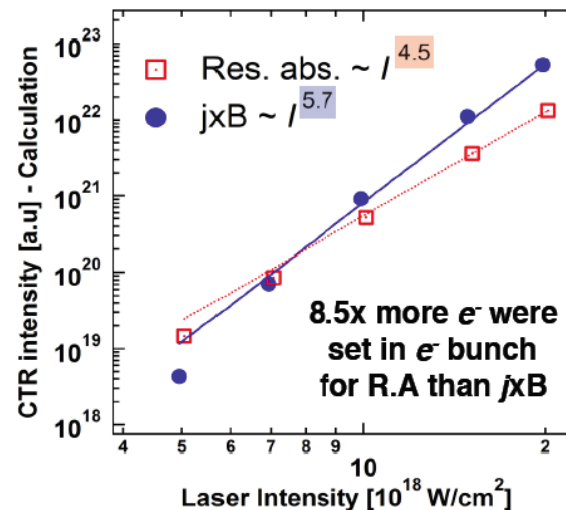
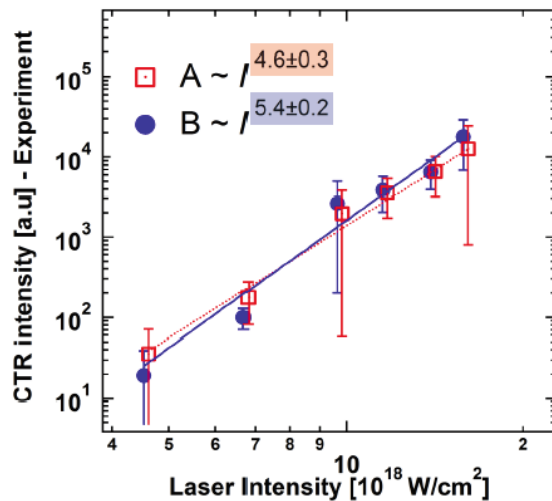
We have identified two hot electron generation mechanisms at work simultaneously on planar targets



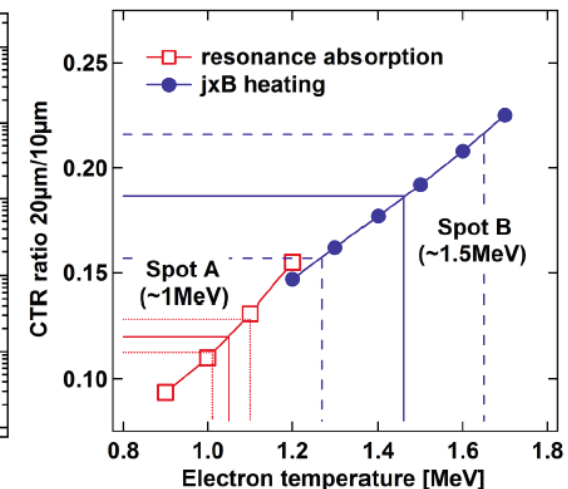
$2\omega_0$ CTR from 10 μm aluminum foil



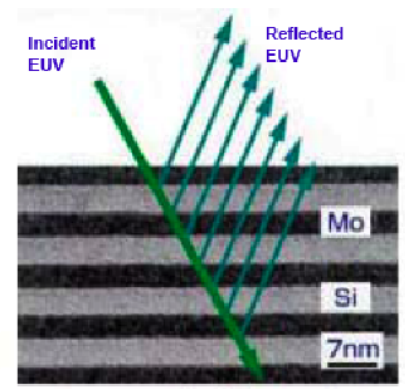
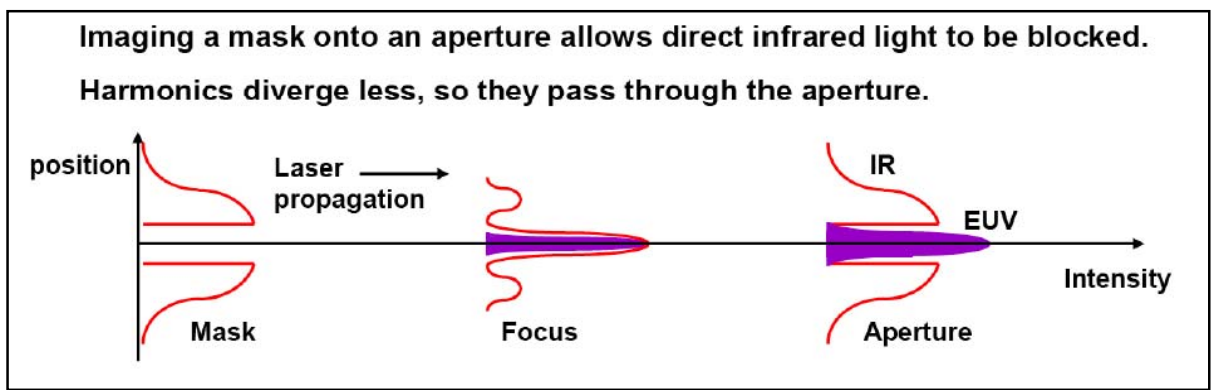
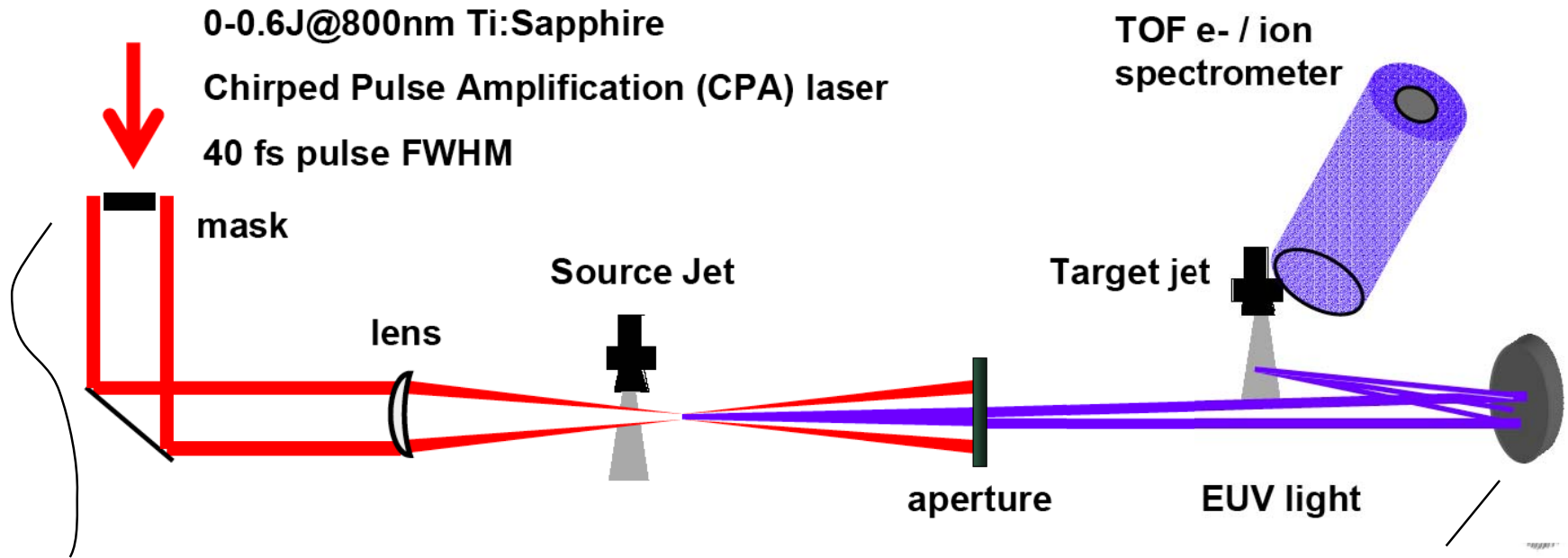
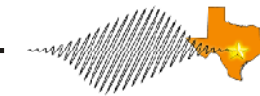
CTR vs I , measurement & calculation



CTR ratios (20 / 10 μm foils) & T_e



We use the THOR laser to generate harmonics in the ~30 nm region and refocus them into a cluster jet

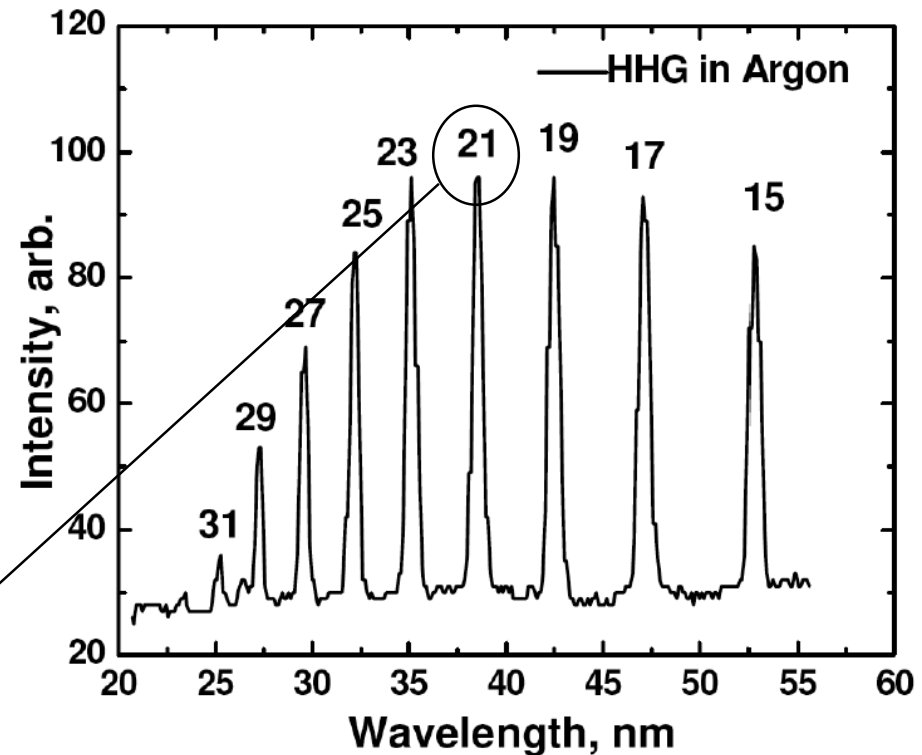
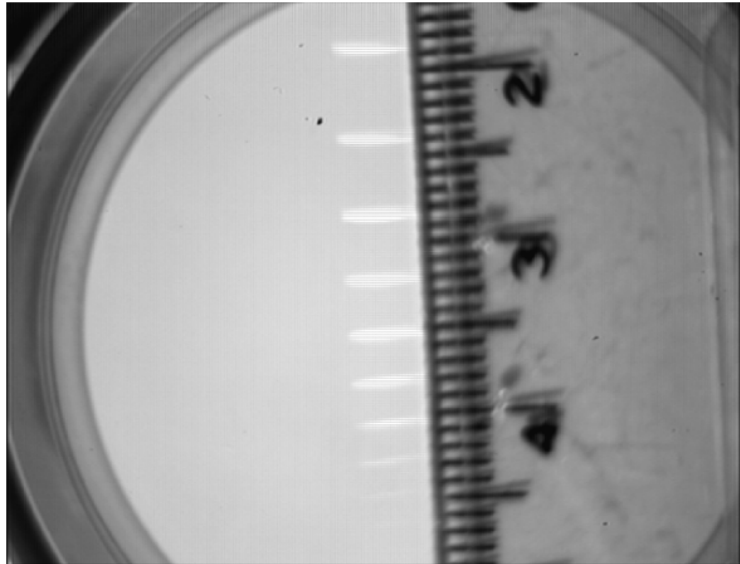
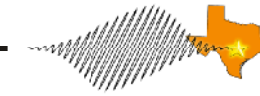


Cross sectional image of Mo/Si multilayer mirror and EUV reflection mechanism. (IOF Fraunhofer, Jena)

Multilayer mirrors are $\lambda/4$ stacks, with periodicity $\sim 10\text{nm}$.
 Sc/Si mirror reflectivity $R \sim 0.3-0.5$ in the 35-50nm region.

-Uspenskii, Vinogradov et. al.,
 Optics Letters 20, 771 (1998)

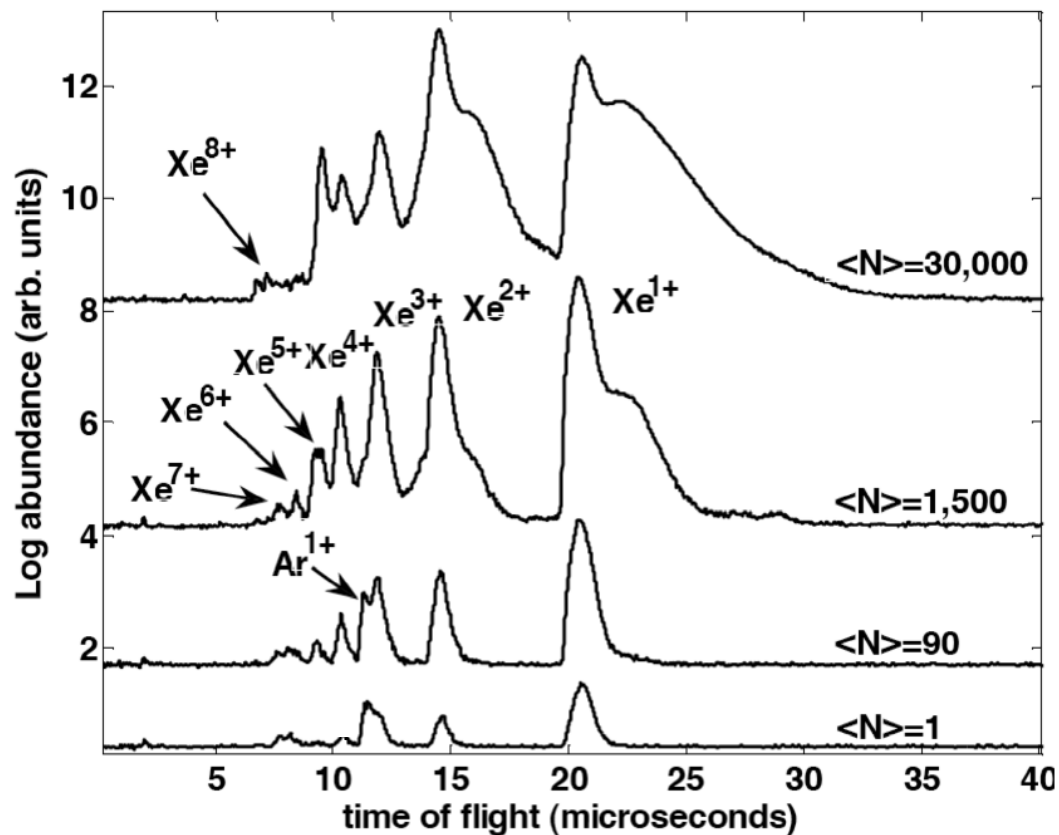
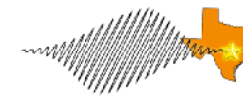
We generate 32.7 eV pulses by high harmonic generation in argon



Harmonic selected for these experiments: $h\nu = 32.7$ eV ($\lambda = 38$ nm)

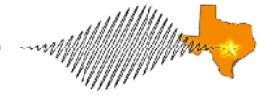
XUV photo diode measurements indicate that we focus ~ 1 nJ of 38 nm light into the Xe cluster jet

High charge states are produced when Xe clusters of > 1000 atoms are irradiated

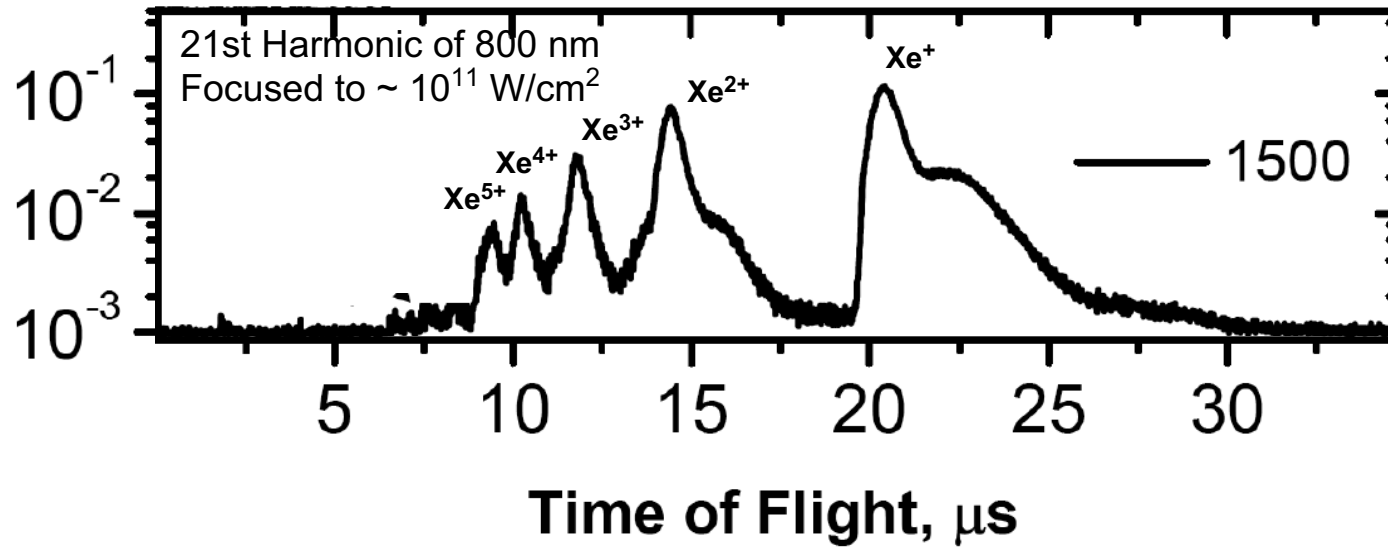


Efficient production of charge states of up to 5+ are observed, with some evidence for charge states up to 8+

The high charge states observed in Xe clusters are anomalous



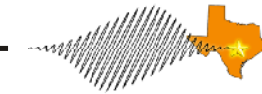
Exploding Xe cluster TOF spectrum



$$h\nu_{q=21} = 32.6 \text{ eV}$$

<u>Charge state</u>	<u>Ionization Potential</u>
Xe ⁰	12.1 eV
Xe ⁺¹	21.2 eV
Xe ⁺²	32.1 eV
Xe ⁺³	46.7 eV
Xe ⁺⁴	59.7 eV
Xe ⁺⁵	71.8 eV
Xe ⁺⁶	92.1 eV
Xe ⁺⁷	105.9 eV

Continuum lowering coupled with photoionization may explain our observed charge states



Exploding Xe cluster TOF spectrum

